Aalto University
School of Chemical
Technology

School of Chemical Technology
Degree Programme of Chemical Technology

Sanna Renkonen

REMOVAL OF ALKALI METALS FOR THE ENHANCEMENT OF FAST PYROLYSIS PROCESS

Master's thesis for the degree of Master of Science in Technology submitted for inspection, Espoo, 26 August, 2016.

Supervisor **Professor Pekka Oinas**

Instructors **PhD Anja Oasmaa and DSc Sarwar Golam**

Aalto University
School of Chemical
Technology

Aalto University, P.O. BOX 11000, 00076 AALTO
www.aalto.fi
Abstract of master's thesis

Author Sanna Renkonen

Title of thesis REMOVAL OF ALKALI METALS FOR THE ENHANCEMENT OF FAST PYROLYSIS PROCESS

Department Department of Chemical Technology

Professorship Plant Design **Code of professorship** KE-107

Thesis supervisor Professor Pekka Oinas

Thesis advisors/Thesis examiners PhD Anja Oasmaa, DSc Sarwar Golam

Date 26.08.2016 **Number of pages** 95+7 **Language** English

Abstract: Alkali metals have detrimental effects on fast pyrolysis process for bio crude. In this thesis, a new process for the removal of these alkalis was designed. In this way, the yield, quality and profitability of pyrolysis process could be enhanced.

The design of the unit included testing the wash process in laboratory and pilot scale, choosing the suitable equipment, drawing the flow chart including the control instruments, writing the operating instructions, calculating the mass balances, defining the technical values for the equipment. The economic potential of the unit was studied by searching the current prices for the equipment, calculating the fixed capital investment and the operating costs based on the balances and power consumption of equipment and comparing these to the grown sale incomes. Sensitivity analysis was performed for the fixed capital investment and the prices of chemicals: nitric acid and sodium hydroxide.

In this Thesis, a process including the following phases was designed: The forest residue biomass is crushed into a finer particle size (to <5 mm), washed with 40 °C 1 % nitric acid (1:5), solid is separated with vacuum in a rotary vacuum drum washer, rinsed with 40 °C water (1:5), pressed with a mechanical press to remove the residual water and the used acid is neutralized by sodium hydroxide. Water is recycled by reverse osmosis, which separates the salts. The waste water is led to the municipal waste water treatment plant.

The goal of the washing process is to reduce the ash content of the forest residue to the level of trunk tree. The goal was achieved in laboratory scale and fairly in the pilot scale experiment. The ash removal efficiency was 50 % in laboratory and 45 % in pilot scale. However, the pyrolysis experiment showed that the bio-oil yield was only slightly increased, when the washed biomass was used instead of the regular forest residue. At the moment, this process does not have economic potential without major modifications and further study.

Keywords process design, biomass alkali removal, washing process, fast pyrolysis, bio-oil, rotary vacuum drum washer, reverse osmosis, mass balance, sizing, cost evaluate, sensitivity analysis

Aalto-yliopisto
Kemian tekniikan
korkeakoulu

Aalto-yliopisto, PL 11000, 00076 AALTO
www.aalto.fi
Diplomityön tiivistelmä

Tekijä Sanna Renkonen

Työn nimi ALKALIMETALLIEN POISTO BIOMASSASTA NOPEAPYROLYYSIPROSESSIN TEHOSTAMISEKSI

Laitos Kemian tekniikan laitos

Professuuri Tehdassuunnittelu **Professuurikoodi** KE-107

Työn valvoja Professori Pekka Oinas

Työn ohjaajat/Työn tarkastajat Tohtori Anja Oasmaa, tohtori Sarwar Golam

Päivämäärä 26.08.2016 **Sivumäärä** 95+7 **Kieli** englanti

Tiivistelmä: Alkalimetallit vaikuttavat nopeapyrolyysiprosessiin haitallisesti. Tässä työssä suunniteltiin prosessi, jolla poistetaan alkalimetalleja biomassasta. Näin voitaisiin parantaa varsinaisen pyrolyysiprosessin kannattavuutta ja nostaa tuotteen laatua.

Alkalinpoistoyksikkö suunniteltiin testaamalla pesuprosessia laboratoriossa ja pilot-mittakaavassa, valitsemalla sopivat laitteet, piirtämällä virtauskaavio säätöventtiileineen, kirjoittamalla käyttöohjeet, laskemalla ainetaseet, määrittämällä tärkeimmät tekniset arvot kaikille laitteille. Yksikön taloudellinen kannattavuus selvitettiin etsimällä ajankohtaiset hinnat laitteille, laskemalla hankintameno näiden perusteella, laskemalla käyttökustannukset ainetaseiden perusteella sekä laitteiden sähkönkulutus ja vertaamalla näitä kasvaneisiin myyntituloihin. Herkkyysanalyysi tehtiin investointi- ja käyttökustannuksille.

Työssä suunniteltiin prosessi, jossa on seuraavat vaiheet: Metsätähdebiomassa murskataan hienompaan partikkelikokoon (< 5 mm), pestään 40 °C:lla laimealla typpihapolla (1:5), kiintoaine erotetaan alipaineessa rummussa, huuhdellaan 40 °C vedellä (1:5), puristetaan kosteus pois mekaanisella prässillä ja käytetty happo neutraloidaan lipeällä. Suurin osa vedestä kierrätetään käänteisosmoosilla, joka erottelee suolat. Jätevesi johdetaan kunnalliselle jätevedenpuhdistamolle.

Pesuprosessin tavoitteena on vähentää biomassan tuhkapitoisuus runkopuun tasolle. Tavoite saavutettiin laboratoriossa ja lähes saavutettiin pilot-kokeessa. Poistotehokkuus oli 50 % laboratoriossa ja 45 % pilot-kokeessa. Bioöljyn orgaanisen nesteen saanto pestyn biomassan pyrolyysikokeessa (56 %) ei kuitenkaan merkittävästi poikennut saannosta pesemättömälle raaka-aineelle (53 %). Prosessi ei ole taloudellisesti kannattava ilman merkittäviä muutoksia ja jatkotutkimusta.

Avainsanat prosessisuunnittelu, biomassan alkalin poisto, pesuprosessi, nopea pyrolyysi, bioöljy, rumpupesuri, käänteisosmoosi, massatase, mitoitus, kustannusarvio, herkkyysanalyysi

Acknowledgements

This thesis was written at VTT during the 2016 spring semester and summer. I am very thankful for the opportunity to work with the top experts in the field and the possibility to learn about chemical technology and plant design.

I thank my advisor, Anja Oasmaa, for the discovery of the interesting research idea. I am also thankful for my colleagues (Yrjö Solantausta, Christian Lindfors, Kristian Melin and the others) and supervisors (Pekka Oinas and Sarwar Golam) for giving me good advice in the field of chemical process technology and in the writing process of the thesis. I am very thankful for my assistants, Elina Paasonen and Juha Tähtiharju, for the proficient and enthusiastic performance of the laboratory and pilot scale experiments. I thank my chemist friends for the career support, and my family and relatives for the life-long backup.

Table of contents

List of symbols

A = area (m^2)

b = biomass binds the liquid b-fold

c = capacity (t/m^2) or (t/h) or (m^3/h) depending on the case

C = cost (k€)

c_p= specific heat capacity $\left(\frac{\mathrm{kJ}}{\mathrm{kg \cdot K}}\right)$

d = diameter (m)

E = energy consumption (kWh)

f_d = discounting factor

g = gravitational acceleration (m/s^2)

h = height (m)

H = head of a pump (m)

l = length (m)

$\dot{m}$ = mass flow $\left(\frac{\mathrm{kg}}{\mathrm{s}}\right)$ or $\left(\frac{\mathrm{t}}{\mathrm{h}}\right)$ depending on the case

M = molar mass $\left(\frac{\mathrm{g}}{\mathrm{mol}}\right)$

n = amount of substance (mol)

η = efficiency

Δp = pressure difference (Pa)

p = water permeability

P = power (kW)

r = rejection of dissolved ash

ρ = density (kg/m^3)

r = radius (m)

s = speed (rpm)

ΔT_{LM} = logarithmic mean temperature difference (°C)

t = time (s)

T = temperature (°C)

U = heat transfer coefficient (W/m^{2}K)

V = volume (m^3)

$\dot{V}$ = volume flow $\left(\frac{m^3}{s}\right)$

W = width (m)

w = mass fraction

φ = flux $\left(\frac{m^3}{m^2 \cdot day}\right)$

1 Introduction

1.1 Background

These days a growing interest in energy research is directed towards renewable energy sources, because fossil fuel resources are limited and the total CO_2-emissions should be reduced. One of the most interesting renewable fuels is fast pyrolysis bio-oil (FPBO), which is produced from biomass by fast pyrolysis. Bio-oils may be utilized, stored and shipped much like conventional liquid fuels once their specific properties are taken into account (Oasmaa et al. 2010b). The use of bio-oil reduces greenhouse gas emissions over 90 % compared to fossil fuels (Fortum 2015) and gives an opportunity to energy industry to become more self-sufficient.

Valmet has built in Joensuu the world's first integrated fast pyrolysis plant for Fortum in 2013. This CHP-plant (*combined heat and power plant*) produces 50 000 tons of bio-oil from forest residue biomass annually in addition to heat and power. 50 000 tons of bio-oil can heat more than 10 000 households a year. (Fortum 2015) The plant utilizes VTT's (*Technical Research Centre of Finland*) integrated pyrolysis technology, which is further developed in the Bioruukki pilot centre, PDU. The raw material and product of the fast pyrolysis from PDU are presented in Figure 1. In the future bio-oil may perhaps be used also for the production of traffic fuels and biochemicals. More than 200 organic chemicals could be produced from pyrolysis oil (Scholze 2002).

Figure 1. Raw material and product of fast pyrolysis from PDU

The quality, yield and price of bio-oil could be increased by developing a process for the alkali removal. Alkalis in biomass cause a lot of problems in the fast pyrolysis plant. Alkali metals decrease bio-oil yield in fast pyrolysis (Oasmaa et al. 2010a, Trendewich et al. 2015), cause phase-separation of fresh bio-oil (Oasmaa et al. 2015a) and poison catalysts in catalytic pyrolysis (Paasikallio et al. 2014). Alkali metals in biomass cause also higher particulate emissions in the bio-oil combustion (Jiménez et al. 2006) and maintenance problems such as sintering, fouling and corrosion in thermal conversion plants. These processes reduce the efficiency and availability of these plants and increase operation costs. (Turn et al. 1997, Davidsson et al. 2002) These problems could be reduced by removing the alkalis from biomass. The yield increase of organic liquid is especially significant, when lower grade feedstocks containing high amounts of ash, such as forest residue biomass, are used in the production of the fast pyrolysis bio-oil.

The focus in this thesis will be on the method, which combines acid wash and water rinsing for the biomass alkali removal. This thesis is a part of Tekes High Demand -project at VTT, in which also other possible biomass alkali removal methods have been investigated. Those include hot-filtration of vapours, ion-exchange of bio-oil, filtration, centrifugation and steam explosion.

1.2 Aim of thesis

There are two aims in this thesis. The first goal is to design a realistic and functioning biomass alkali removal process for the fast pyrolysis plant. Another objective is to study the economic potential of that process.

These goals will be reached by testing the wash process both in laboratory and pilot scale, choosing the suitable equipment for the process, drawing the flow chart including the control instruments, calculating the mass balances based on the laboratory experiments, defining the most important dimensions and specifications for all the equipment and writing the operating instructions for the function of the new unit. The economic potential will be studied by searching the current prices for all equipment, calculating the fixed capital investment based on these, calculating the annual operating costs of the unit based on the balances and power consumption of equipment and calculating the sale incomes. In addition, the sensitivity analysis is performed for the fixed capital investment and the chemical (HNO_3 and NaOH) prices.

All the calculations, dimensions and equipment for the biomass alkali removal unit are designed in the same size scale as the Fortum's plant presented in Chapter 2.1. However, Fortum's plant is used here only as an example and the plant performance is based on published data.

LITERATURE PART

2 Process for alkali removal

2.1 Commercial fast pyrolysis process

There are three commercial scale fast pyrolysis demonstration plants in the world. They are located in Joensuu, Finland (Fortum 2015), in Hengelo, the Netherlands (Empyro 2015) and in Renfrew, Canada (Bradley 2015). Even though the reactor technology differs, the principle of the process is similar in each plant, and there are not significant differences in product yields or quality. Consequently, it is sufficient to present only one and Fortum's plant is used here as an example.

Currently the market price (€/MJ) of the bio-oil may be considered similar as the market price of heavy fuel oil, HFO. The market price of the new bio-oil is something between that of the light fuel oil, LFO, and that of HFO. However, large variation in the oil prices has occurred during the past decades. The heavy fuel oil prices in Rotterdam, light fuel oil prices in Finland and forest residue fuel prices in Finland are presented in Figure 2.

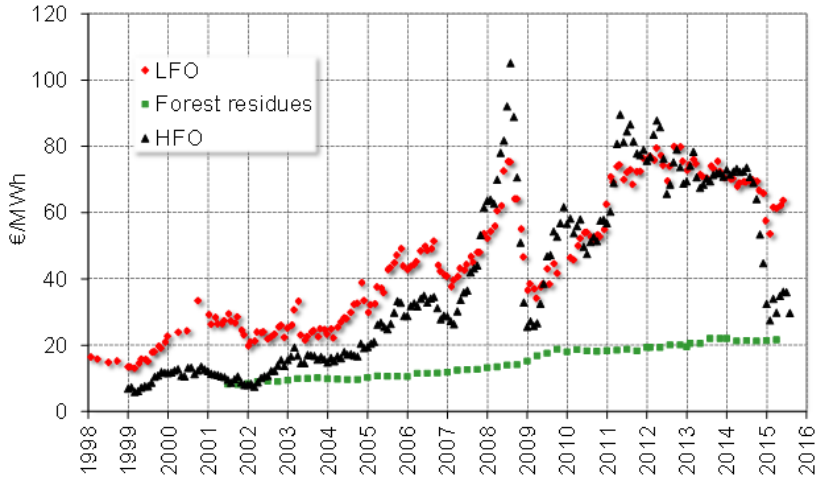

Figure 2. Heavy fuel oil prices in Rotterdam (Insee 2016), light fuel oil prices in Finland and forest residue fuel prices in Finland without taxes (Tilastokeskus 2015).

Thermal fast (or flash, rapid) pyrolysis is a process, in which biomass is heated rapidly (<2 s) to about 500 °C at an inert atmosphere. Biomass is converted into vapors and char. The non-pyrolyzed wooden part, char, is removed in cyclones. The vapors are condensed into product liquid, which is called fast pyrolysis bio-oil. The non-condensed gases are used for heating and fluidization. Typical yields from bark-free wood are 62 w-% organic liquid, 12 w-% pyrolysis water, 14 w-% char and 12 w-% gas on dry feed (Solantausta et al. 2012). Yields of the products obtained from fast pyrolysis depend strongly on the physical and chemical nature of the feed, but also on the reaction parameters, the reaction system temperature and reaction time. The obtained by-products gas and charcoal can be used to dry the feed and to preheat the reactor. (Bridgwater et al. 1999, Scholze 2002)

In the Fortum's integrated fast pyrolysis plant, fast pyrolysis bio-oil is produced as presented here. The raw material is forest residue biomass, which consists of wood chips, saw dust and other wood-based forest residue biomass. The process begins with drying of the raw material with a belt dryer. Hot air is used for

drying. (Fortum 2015) There are three different sources for the hot air: heat from the condensation of the pyrolysis oil, steam from the turbine and district heat. The heat from the condensation of the pyrolysis oil is attempted to utilize as much as possible, because it is free waste heat from the process (Solantausta 2016). After drying the wood chips have a moisture content of about 8 w-%. Subsequently the raw material is milled to finer particles. This is carried out in the fine milling unit of the process. The milled raw material is transported to the pyrolysis reactor. Before the pyrolysis, the fuel is stored in a reactor fuel silo. (Fortum 2015) After the pyrolysis reaction the purge gas is supplied to the fluidized bed boiler, which has a temperature of 800 °C. The sand and char are also fed to the fluidized bed boiler. In the integrated fast pyrolysis/CHP plant, two products in different units are manufactured: bio-oil, and high pressure steam from the fluidized bed boiler, from which heat and electricity can be produced. The produced bio-oil is pumped into a storage tank. Bio-oil can be utilized for example as a conventional fuel in district heat boilers. Electricity, 55 MW, and district heat, 110 MW, are produced from the high pressure steam with a turbine. (Fortum 2015)

2.2 Properties of biomass

There are many different types of biomass, but in this thesis we refer to wood-based biomass, to lignocelluloses. The major components in wood are cellulose, hemicelluloses and lignin. These three components form about 95–97 w-% of dried wood. There are also neutral substances, extractives, in the wood, especially when bark and needles are present. The rest is inorganics. About 42 % of the mass of dried wood consists of cellulose. Hardwood and softwood consist of 16–24 % and 24–33 % of lignin, and about 30–38 % and 21–30 % of hemicellulose, respectively. (Scholze 2002) In Finland, the total volume of growing stock consists of pine (46 %), spruce (37 %), birch (14 %) and other wood (3 %) (Kaipainen 2003). Pine and spruce are classified as softwood, birch as hardwood. Fresh wood moisture content is usually in the range of 40–60 %

(Alakangas 2000). The elemental composition of forest residue chips in Finland is presented in Table 1. The logging residue chip size is presented in Figure 3.

Table 1. Elemental composition of forest residue on dry basis, d.b, in Finland (Alakangas 2000, Wilén et al. 1996).

Ultimate analysis (w-% d.b.)						Moisture
C	H	N	O	S	Ash	[%]
48–52	6.0–6.2	0.3–0.5	38–42	<0.05	1.3	40-60

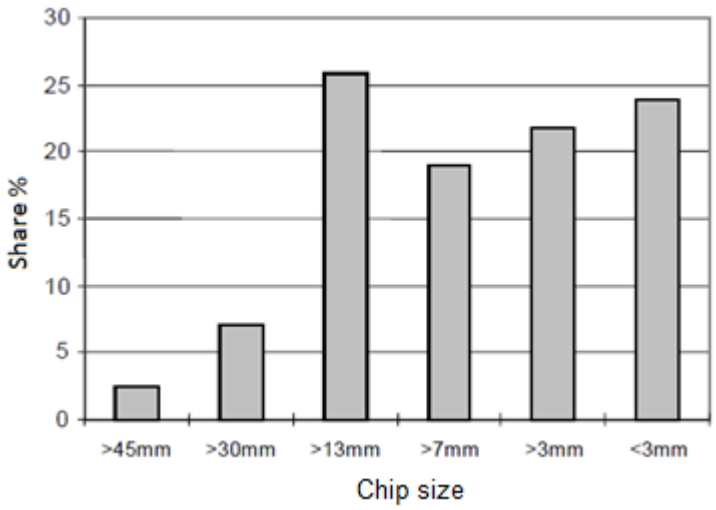

Figure 3. Logging residue chip size. Moisture percent of logging residue varies between 25–65 w-%. (Alakangas 2000)

2.3 Alkalis in biomass

The most important alkali- and alkaline earth metals, AAEMs, in biomass are K, Na, Ca and Mg. The compounds of alkalis in biomass occur primarily in the form of silicates (e.g K-Na-Ca-Mg-aluminosilicates), hydroxides (e.g. $Mg(OH)_2$), sulfates (e.g. Na_2SO_4), phosphates (e.g $MgCaPO_4$), carbonates ($CaCO_3$), chlorides (KCl), and nitrates (KNO_3). A comprehensive list of ash compounds in biomass is presented in Attachment 4. (Vassilev et al. 2012) The ash compositions of different biomasses are presented in Table 2.

Large quantities of alkali metals are required as nutrients and counter ions in living plants. For example, in the fast growing parts of trees, such as small branches, twigs and leaves, the alkali contents are higher than in trunk tree and in larger branches. Around 90 % of the alkali in biomass is present in water-soluble or ion exchangeable form and has potential to vaporize during heating. (Davidsson et al. 2002) Potassium is bound in biomass predominantly as salts or organically bound in ion-exchangeable form (Valmari 2000). Nevertheless, little information is available on mineral matter in biomass and the combined qualitative and quantitative determinations are almost missing in contrast to coal (Vassilev et al. 2012).

Table 2. Ash compositions of different biomasses on dry basis (Wilén et al. 1996).

	Ash [w-%]	Ca [g/kg]	Si [g/kg]	K [g/kg]	Al [g/kg]	Fe [g/kg]	Mg [g/kg]	P [g/kg]	S [g/kg]	Na [g/kg]
Alkali metal				X						X
Alkaline earth metal		X					X			
Northern Woody Biomasses										
Forest residue chips Finnish	1.3	110	180	69	25	26	24	14	7	3
Wood chips	0.6	240	110	100	27	15	31	21	7	2
Saw dust (pine)	0.1	300	39	102	11	13	71	23	8	2
Spruce bark	2.3	280	7	63	6	1	31	18	4	3
Pine bark	1.7	290	6	63	28	2	27	21	8	4
Agricultural Biomasses										
Wheat straw (Danish)	4.7	52	280	140	4	4	11	10	4	4
Barley straw (Finnish)	5.9	32	290	160	<1	1	13	11	6	4
Rapeseed	2.9	210	15	140	3	7	4	39	43	3
Flax	2.9	240	17	200	4	4	31	67	15	3

Table 2 indicates that the alkali concentration in bark is significantly higher than that of the trunk tree material, such as wood chips and saw dust. Because of this, the bark could theoretically be separated from the trunk and the alkali removal process performed only for the bark. However, this alternative is not studied in this thesis, because it would include the design of a new chipping and sorting system to the terminal.

Potassium chloride, sodium chloride and potassium hydroxide are highly soluble in water. Potassium phosphate, potassium nitrate, calcium nitrate, sodium sulphate, potassium sulfate and magnesium sulfate are also soluble in water. The solubilities of some alkali compounds are presented in Figure 4. Many examples

on the behavior of alkali compounds in water and acids are presented in Equations 1–13 to clarify the chemistry behind the alkali removal process by washing.

$$KCl(s) \rightarrow K^+(aq) + Cl^-(aq) \quad (1)$$

$$NaCl\ (s) \rightarrow Na^+(aq) + Cl^-(aq) \quad (2)$$

$$KOH\ (s) \rightarrow K^+(aq) + OH^-(aq) \quad (3)$$

$$K_3PO_4(s) \rightarrow 3\ K^+(aq) + PO_4^{3-}(aq) \quad (4)$$

$$Ca(NO_3)_2(s) \rightarrow Ca^{2+}(aq) + 2\ NO_3^-(aq) \quad (5)$$

$$KNO_3(s) \rightarrow K^+(aq) + NO_3^-(aq) \quad (6)$$

$$Na_2SO_4\ (s) \rightarrow 2\ Na^+(aq) + SO_4^{2-}(aq) \quad (7)$$

$$K_2SO_4(s) \rightarrow 2\ K^+(aq) + {SO_4}^{2-}(aq) \quad (8)$$

$$MgSO_4(s) \rightarrow Mg^{2+}(aq) + {SO_4}^{2-}(aq) \quad (9)$$

Calcium hydroxide and oxide react with acids, but are slightly soluble in water. Calcium phosphate and magnesium phosphate are slightly soluble in water, but soluble in acids.

$$Ca(OH)_2(s) + 2\ H^+(aq) \rightarrow Ca^{2+}(l) + 2H_2O \quad (10)$$

$$CaO\ (s) + 2\ H^+(aq) \rightarrow Ca^{2+}(l) + H_2O \quad (11)$$

$$Mg_3(PO_4)_2 + 6\ H^+(aq) \rightarrow 3\ Mg^{2+}(l) + 2PO_4^{3-}(l) + 6\ H^+(aq) \quad (12)$$

$$Ca_3(PO_4)_2 + 6\ H^+(aq) \rightarrow 3\ Ca^{2+}(l) + 2PO_4^{3-}(l) + 6\ H^+(aq) \quad (13)$$

Calcium sulphate is slightly soluble in both water and acids.

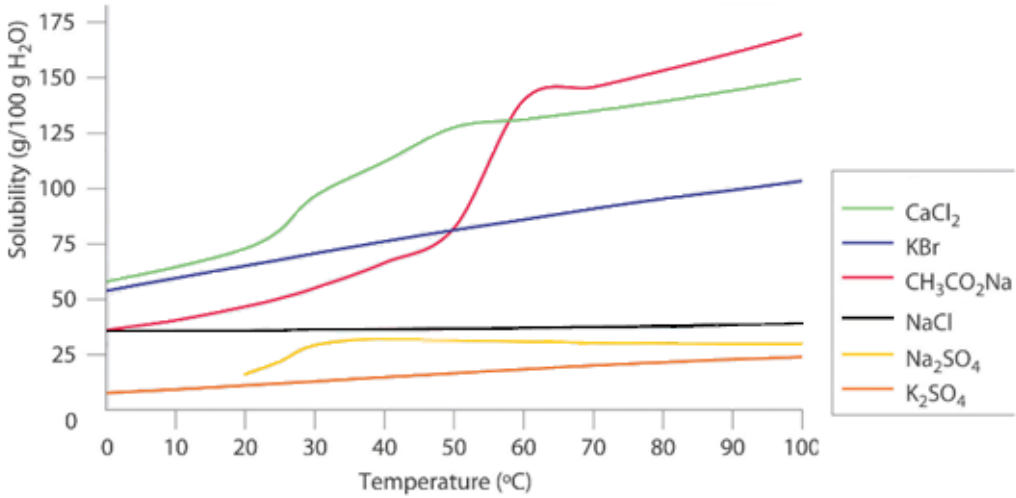

Figure 4. Solubility of some alkali compounds as a function of temperature (Averill 2016).

2.4 Process equipment alternatives

2.4.1 Washing

The biomass alkali removal is a washing process in this thesis. Washing is defined as solid-liquid separation, in which the undesired compounds move from the solid phase to the liquid phase (Alopaeus 2016). Nevertheless, the biomass alkali removal is sometimes referred as “leaching” in literature, which is not correct in this case. That is because leaching is defined as solid-liquid separation, in which the desired compounds move from the solid phase to the liquid phase (Alopaeus 2016), and in this thesis, the utilization of the residual alkalis is not particularly considered.

Chemical processes can be batch or continuous processes. In this case, a continuous/semi batch process was selected, because it is more suitable type for

large scale industrial processes, the sizes of equipment can be smaller, process functions more smoothly, inherent safety is higher and solvent recovery is easier. (Oinas 2016)

Filtration is the most commonly used unit operation for a continuous washing process including the separation of most solvent. The equipment alternatives for continuously washing with filtration are: horizontal belt, rotary vacuum drum washer with bottom feed, rotary table and rotary tilting pan. The rotary vacuum drum washer seems to be the most attractive option for the alkali removal process, because each of the other alternatives has some disadvantages. The horizontal belt occupies large floor space, has relatively high cost of installation per unit filter area and causes a need for good post-treatment. With the rotary tilting pan good washing results could be achieved, but this advantage is offset by its mechanical complexity and high capital cost. The rotary table instead has some operational difficulties including cloth washing difficulties. (Tarleton et al. 2007)

Rotary vacuum drum washer is one of the most typical washer types used in the pulp industry. It consists of a wire mesh covered cylinder, which rotates in a tub of the pulp slurry, and valve arrangements to apply vacuum. The rotating speed is usually about 5 rpm. As the drum contacts the slurry, a vacuum (10 – 85 kPa) is served to thicken the mass. The drum rotates past wash showers. After this the vacuum is cut off and the pulp mat is dislodged. (Biermann 1996, Tarleton et al. 2007)

The principle of the rotary vacuum drum washer is presented in Figure 5. The exterior of a rotary vacuum drum washer is shown in Figure 6. Figure 6 indicates that the mass transfer area covered with the wire mesh is limited to the jacket of the rotary vacuum drum washer.

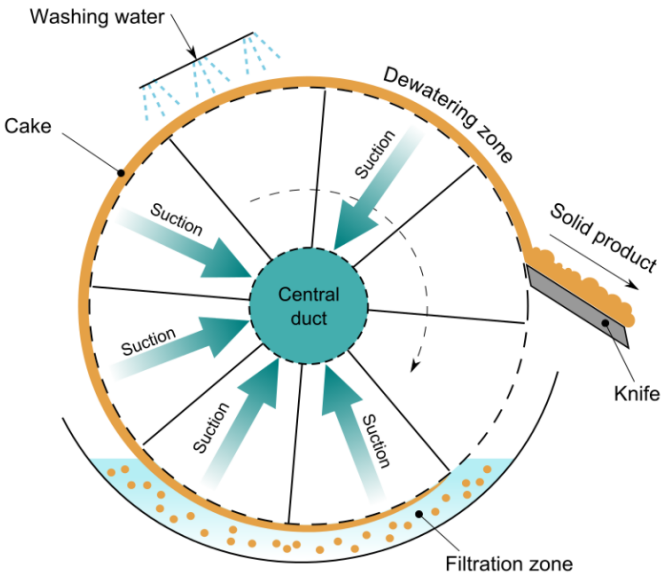

Figure 5. Principle of rotary vacuum drum washer. (Seminarsonly 2015) The vacuum inside the drum sucks the slurry of biomass and washing liquid to the outside surface of a rotating drum. The liquid passes through the cloth and is directed out as the biomass stays on top of the cloth. As the cake keeps rotating, it is rinsed with water, which is also sucked inside the drum with vacuum. Finally, the cake is discharged with a knife for example.

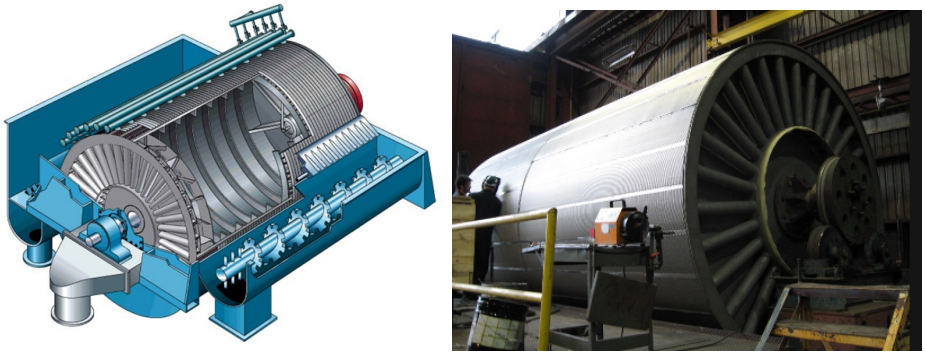

Figure 6. Rotary vacuum drum washer (GL&V 2014).

The advantages of the rotary vacuum drum washer include inexpensive prices, well-known technique and a variety of construction materials available. (GL&V 2014) Hence the rotary vacuum drum washer fulfills the criterion for the biomass washing equipment.

2.4.2 Recycling of water

Most of the dissolved salts should be removed from water, so that the reuse of water will be possible. The removal of dissolved salts can be done using reverse osmosis, RO, which is a membrane separation process. The separation size scale of reverse osmosis (~0.1 nm) is more suitable for this situation than that of nanofiltration (~1 nm) for example. Osmosis is a natural process, in which the solvent moves to the more concentrated side of the semi-permeable porous membrane. In reverse osmosis the solvent is forced to flow to the opposite direction through the membrane with pressure higher than the natural osmotic gradient on the feed side. Simultaneously, the dissolved solids are largely rejected by the membrane. The fractionation of molecules is mostly based on their sizes and shapes. On the other words the permeate solution containing the 'smaller' species penetrates through the membrane, whereas the retentate solution containing the 'larger' species is rejected by the membrane, which can be seen in Figure 7. Reverse osmosis is usually applied for sea water or brackish water desalination, but can be also used for purifying organic solvents. (Bradshaw 1997, McCabe et al. 1993)

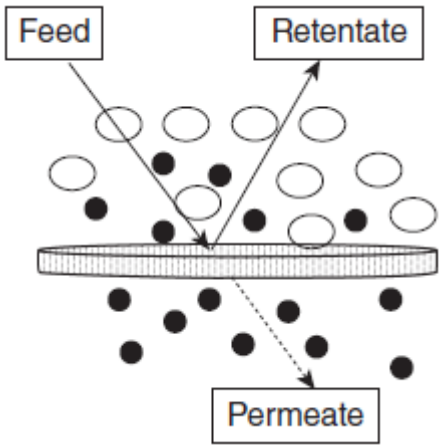

Figure 7. Principle of membrane separation (Datta et al. 2014) such as reverse osmosis.

The advantages of the RO include separations efficiency, environmental friendliness, energy savings, and other economic benefits (Datta et al. 2014). Typical brackish water installations can separate 98 % of the salt from feed water. RO plants have a very high space/production capacity ratio, ranging from 25 to 60 $m^3/day/m^2$ membrane. (Bradshaw 1997) This unit operation can take place at room temperature and there is no phase change, which would require supplying and removing large amounts of energy (McCabe et al. 1993).

The disadvantages of the reverse osmosis include the demand for the regular cleaning of membrane and the high pressure required. Brackish water contains 0.1–3.5 % of salts (Engineering Toolbox 2016a), which is more than fresh water, but less than sea water. The operating pressures range from 17 to 28 bar for brackish water desalination. The operating pressures for sea water desalination are much higher (55–70 bars). (Bradshaw 1997) Luckily, the salt concentrations of the used liquid in this process are a lot closer to the brackish water salt concentrations, see Chapter 6.2.6. Some of the pressurizing energy can be recovered with a turbine, so the thermodynamic efficiency of the process is relatively high (McCabe et al. 1993).

2.4.3 Separation of residual water

The biomass and the residual water are separated after the washing. The separation should be done as cost-efficiently as possible. The solid-liquid-separation in industry can be done using various methods, including thermal heating, pressing, gravity, filtration, cyclones, centrifuges and membranes (Tarleton et al. 2007). The mechanical pressing of the biomass seems to be the most attractive option, because it is a simple and cost-efficient unit operation.

Stefan Sobota (2014) has invented an especially efficient industrial mechanical press for the separation of biomass and water. The pressing with this equipment can remove even half of the water naturally bound to biomass (see Chapter 6.1.1). Naturally biomass has the moisture content of 40–60 % (Alakangas 2000). The moisture distribution in biomass after pressing will be very uniform also, which facilitates the favorable control of a subsequent process. Large savings in the energy consumption could be achieved by using this equipment after the biomass washing process and before thermal heating in the fast pyrolysis plant (Mynewsdesk 2014, Sobota 2014). Theoretically, energy savings could be achieved even from the current drying costs. The mechanical press for biomass dewatering is presented in Figure 8.

Figure 8. Mechanical press for biomass dewatering (Mynewsdesk 2014).

2.5 Washing experiments in literature

Davidsson et al. (2002) noticed that washing wheat straw, wood waste and cellulose biomass with acetic acid as 1 M solution and rinsing it with water afterwards was a lot more efficient in the alkali removal than washing the biomass only with water. Washing with water reduced the alkalis from wood waste biomass 5–30 % while acid washing was more effective and reduced the alkalis about 70 %. Water and acetic acid were used at room temperatures in the experiments. The ratio of biomass–acetic acid solution was 1:50 and biomass–rinsing water ratio 1:100 in the acid washing. (Davidsson et al. 2002)

Oudenhoven et al. (2013) investigated pine wood washing with second condenser liquid prior to pyrolysis of the biomass. They managed to effectively remove the alkali ions initially present in biomass, as their best removal efficiency of the ash of pine wood was over 96 %. The decreases of ash content in the experiments are presented in Table 4. No significant consumption of acetic acid during the washing step was observed. Rinsing the biomass after acid

washing was noticed to be important in the removal of the washing liquid containing the dissolved minerals. The composition of condensate used in the process is presented in Table 3. Fast pyrolysis of pine wood washed with second condenser liquid combined with rinsing resulted in an increase in organic oil yield and was accompanied with a decrease in water and char yields, as can be noticed in Table 5. The process conditions in these experiments were T_{Wash} = 90 °C, P_{Wash} = 1 bar and t_{Wash} = 120 min. The mass ratio of the washing liquid and the biomass was 10:1. The temperature of the washing liquid was the most critical parameter in the ash removal process, whereas the reaction time was of less importance, which can be seen in Table 4. They noticed also that the ash remaining after washing process was mostly silica. (Oudenhoven et al. 2013)

Table 3. Composition of condensate used in ash removal (Oudenhoven et al. 2013).

	Concentration (mass%)	
	Condenser 2 solution	Synthetic solution
Acetic acid	9.5	10
Acetol	7.6	–
Ethanol	–	3.75
Acetone	–	3.75
Propionic acid	1.4	1.5
Guaiacol	1.7	1.5
Other organics	19.5	
Water	60.5	79.5 (demineralized)

Table 4. Decreases of ash content when different process parameters are tested (Oudenhoven et al. 2013).

Acid solution	Temperature (°C)	Process time (min)	Rinsing	Ash content (wt%)
Untreated				0.53
Synthetic condenser 2 liquid	30	10	Yes	0.49 (0.51/0.47)
Synthetic condenser 2 liquid	30	120	Yes	0.28 (0.26/0.29)
Synthetic condenser 2 liquid	90	10	Yes	0.09 (0.09/0.09)
Synthetic condenser 2 liquid	90	120	Yes	0.04 (0.02/0.05)
Real condenser 2 liquid	90	120	Yes	0.02
Real condenser 2 liquid	90	120	No	0.14

Table 5. Product yields, when following process parameters are used: T_{Wash} = 90 °C, P_{Wash} = 1 bar and t_{Wash} = 120 min. (Oudenhoven et al. 2013)

	Untreated	Cond 2 synthetic	Cond 2 real
Organic yield (kg/kg dry biomass × 100%)	48.2	58.0	56.2
Water yield (kg/kg dry biomass × 100%)	11.9	8.6	6.5
Char yield (kg/kg dry biomass × 100%)	10.2	8.6	8.7
Gas yield (kg/kg dry biomass × 100%)[a]	29.7	24.9	29.8

In another paper, Oudenhoven et al. have listed the removal efficiencies of individual pine wood biomass alkali compounds, which are presented in Table 6. The washing conditions were the same as in their previous study (Oudenhoven et al. 2015).

Table 6. Biomass alkali compounds before and after acid washing. Process conditions were: T_{Wash} = 90 °C, P_{Wash} = 1 bar and t_{Wash} = 120 min. (Oudenhoven et al. 2015)

	Pine	
	Initial	Acid leached
(mg cation/kg dry biomass)		
Na^+	60	2
K^+	398	9
Mg^{2+}	387	9
Ca^{2+}	1771	68
Sum (AAEMs)	**2626**	**88**

Table 6 shows that Oudenhoven et al. (2015) managed to remove 97 % of Na^+, 98 % of K^+, 98 % of Mg^{2+} and 96 % of Ca^{2+}, and the total removal of alkalis was 97 % by acid washing.

Stefanidis et al. (2015) studied pine wood washing with water, 1 % acetic acid and 1 % nitric acid. They used a temperature of 50 °C in all experiments and a reaction time of 4 hours for the water washing and 2 or 4 hours reaction time for the acid washings. They remarked that the most important factor during the biomass pre-treatment was the washing temperature; higher temperatures (50 °C) were significantly more effective for the removal of the inorganics than room temperature. The residence time had a substantially smaller effect on the removal. The biomass loss was not larger in the nitric acid wash than in the acetic acid wash. The ash contents of the initial, the water-washed and the acid-washed pine wood biomasses and the ash removal efficiencies of the washes are presented in Figure 9. The concentrations of K, Na, Mg, Fe, Al, Ca and P before and after washing with water or acid are reviewed in Table 7 and the removal efficiencies of those elements in the same conditions are presented in Figure 10. Figure 10 shows that potassium, sodium and phosphorus were easy to remove, while magnesium, calcium, iron and aluminum were more difficult. The

demineralized biomass samples yielded in increased organic liquid product and reduced char and gas products, especially CO_2. The effect of nitric acid concentration and temperature on the ash removal is presented in Table 8. The influence of acetic acid concentration and temperature on the removal is presented in Table 9. The biomass loss with different washing liquids and concentrations is presented in Table 10. (Stefanidis et al. 2015) Tables 8–9 show that the nitric acid is more efficient washing liquid for the ash removal than acetic acid. Table 10 shows that the biomass loss in dilute nitric acid washing does not differ much from the biomass loss with dilute acetic acid washing.

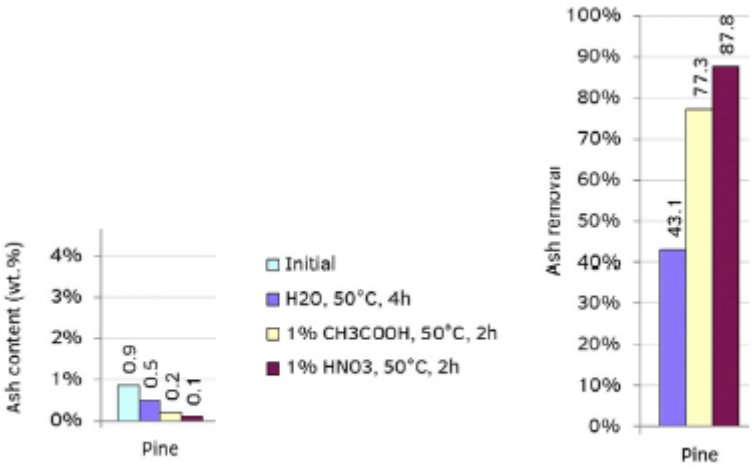

Figure 9. Left: Ash content of initial, water-washed and acid-washed pine wood biomass. Right: Ash removal percent of water washing and acid washing. (Stefanidis et al. 2015)

Table 7. Concentrations of K, Na, Mg, Fe, Al, Ca and P before and after washing with water or acid. Acids were 1-% solutions. Washing temperature was 50 °C. (Stefanidis et al. 2015)

Biomass sample	Treatment	Concentration (ppm on dry biomass)						
		K	Na	Mg	Fe	Al	Ca	P
Pine	Untreated	1049	36	425	287	167	1732	151
	H_2O	118	0	295	249	108	1571	0
	HNO_3	0	0	0	112	68	0	0
	CH_3COOH	0	0	0	239	78	506	0

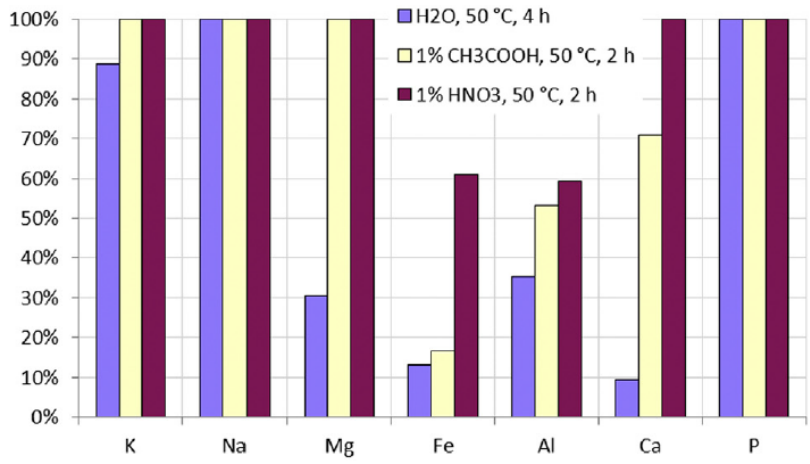

Figure 10. Removal efficiencies of each element after treatment of pine wood with water, acetic acid solution and nitric acid solution (Stefanidis et al. 2015).

Table 8. Effect of nitric acid concentration and temperature on ash removal % (Stefanidis et al. 2015)

Washing liquid HNO_3		
	v-%	
T [°C]	0.1	1
20	72	90
50	85	92

Table 9. Effect of acetic acid concentration and temperature on ash removal % (Stefanidis et al. 2015)

Washing liquid CH_3COOH		
	v-%	
T [°C]	0.1	1
20	52	70
50	60	73

Table 10. Biomass loss with different washing liquids and concentrations, v-% (Stefanidis et al. 2015)

	Biomass loss [%]	
v-% [%]	HNO_3	CH_3COOH
0.1	5	3
1	5	8

2.6 Washing experiments at VTT

In 2013, some laboratory experiments were carried out at VTT on the biomass washing (Oasmaa et al. 2015b). The biomass was washed with condensate from the VTT pilot to remove the ash of the biomass. Forest residue (0.55–0.92 mm, ash content 2.25 w-%) was kept in the condensate for four hours and subsequently rinsed with water as presented in Figure 12. It indicates that biomass-to-condensate mass ratio was 1:10 and biomass-to-rinsing water mass ratio 1:50. The ash content of the biomass was reduced from 2.3 w-% to 0.9–1.3 w-%, so the removal efficiency of ash was 42–60 %. The measured reduction of ash in biomass corresponds to increasing organic liquid yield from 50 to about 58 %, which can be seen from Figure 11. The reasons for the yield increase are based on the reaction kinetics for example. Trendewich et al. (2015) noticed that potassium inhibits the formation of pyrolysis products and catalyzes char formation. Nevertheless, the removal of very small quantities of AAEMs may not result in yield changes, but in all cases will result in modifications of bio-oil composition (Mourant et al. 2011).

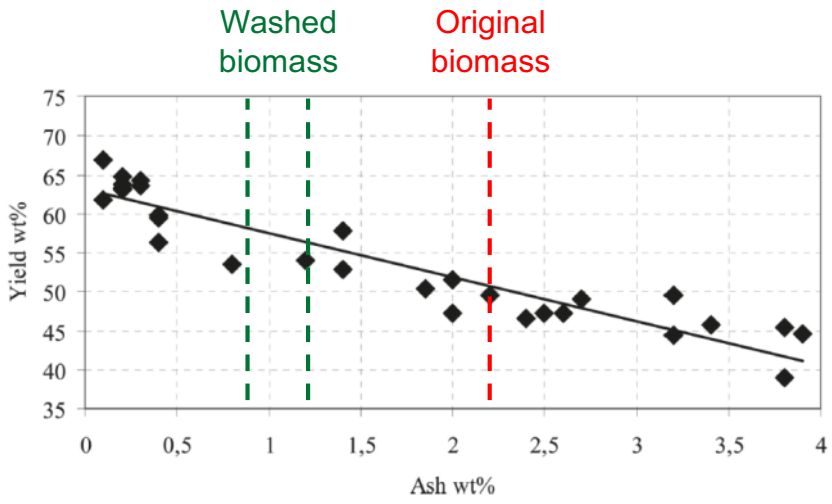

Figure 11. Effect of ash content to yield of bio-oil organics (Oasmaa et al. 2015b).

The conclusions from this experiment were that the removal of ash from feedstock can be feasible:

-If product bio-oil is 10 % more valuable than base oil, and the additional investment is less than about 5 M€ (Oasmaa et al. 2015b).

-If product bio-oil is 20 % more valuable than base oil, and the additional investment is less than about 12 M€ (Oasmaa et al. 2015b).

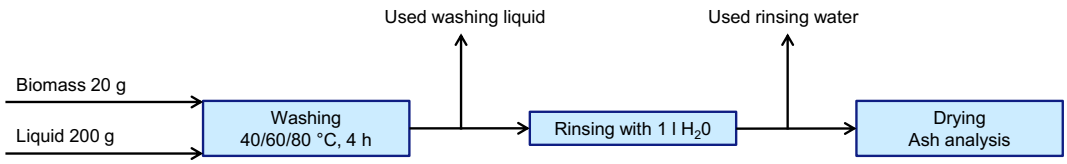

Figure 12. Schematic presentation of biomass washing experiments at VTT.

Another experiment of the biomass wash with acidic waste water was performed at VTT also. The biomass was kept in the acidic liquid 24 hours at 38 °C and then rinsed with water. This washing procedure reduced the ash content of the biomass from 2.3 w-% to 0.5 w-%. This corresponds to 78 % removal. The biomass-to-washing liquid mass ratio was 1:25 in this experiment. Thus, the extended reaction time and the increased amount of washing liquid provided good results. In both of these VTT laboratory experiments, the used biomass was dry. The hypothesis is that the use of wet biomass would decrease the amount of the required washing liquid. The reason for this is that the wet biomass binds the liquid less and the alkalis in the wet biomass could be in a more easily soluble form.

APPLIED PART

3 Laboratory experiments

3.1 Experimental plan

The biomass ash removal in a small scale will be tested in these laboratory experiments. The removal is a phenomenon, which is affected by many different parameters. Even though the subject has been studied previously, it is unclear which parameters affect the removal the most, because contradictory results have been presented (see Chapters 2.5–2.6). Therefore, the effect of many parameters will be explored. Those will be the washing liquid (condensate or nitric acid), the biomass-to-washing liquid mass ratio, the biomass-to-rinsing water mass ratio, the temperature, the residence time and the chip size.

One parameter is changed in every series. Other parameters have the values of a basic point (see Chapter 3.2). The guesses of the parameter values are based on the preliminary mass balance calculations and on the washing experiments in literature (see Chapter 2.5) and the previous experiments at VTT (see Chapter 2.6).

However, the experimental plan was partly altered from the original plan. Since the condensate wash did not function well enough, the nitric acid was selected as the washing liquid for the rest of the experiments. Also the last experimental series was performed with the optimal parameters instead of the basic point parameters, because the data from the removal with the parameters used in the balance calculations was desired.

The purpose of the experimental part is to support the applied part, more precisely, to find the optimal data point for the balance calculations. For this reason, there are extra data points for the most part in the experimental series.

The growth or decrease of the removal efficiency is not necessarily linear as a function of the parameters.

The purpose of the first experimental series was to solve the optimal dilution of the condensate. The object of the second experimental series was to investigate the effect of the temperature to the biomass alkali removal with condensate. The goal of the third and fourth experimental series was to determine the optimal amount of nitric acid solution. The purpose of the fifth experimental series was to investigate the different residence times and the sixth experimental series to study the biomass-to-rinsing water mass ratios. The aim of the seventh experimental series was to study the effect of the particle size of biomass in the ash removal.

Particularly high temperatures for the nitric acid wash will not be tested in this thesis, because the combination of vacuum and high temperature forms a risk of gas generation (see Chapter 3.3). Moreover, the district heat return water used for the heating has a temperature of 60 °C (Solantausta 2016) (see Chapter 6.2.8). Hence the possible washing temperature cannot be too high, to avoid too large heat exchangers. However, it is recommended to investigate the higher temperatures, since good results have been indicated in literature (Oudenhoven et al. 2013, Oudenhoven et al. 2015). Concentration of nitric acid was not tested in this thesis, because Stefanidis et al. 2015 had already defined an optimal value: 1%.

3.2 Experimental setup

Wet forest residue biomass was washed with diluted condensate or with dilute nitric acid solution (1 %) and rinsed with tap water (40 °C). The composition of the condensate is presented in Attachment 3. The experiment was performed as follows:

-The washing liquid was heated to a constant temperature with a plate heater.

-The biomass was added and the mixing was turned on using a magnetic stirrer.

-The biomass-washing liquid slurry was filtered with a suction filter after a specific residence time. Vacuum was used for the suction. Filter paper was not used in the suction process. A Buchner funnel of diameter 9.8 cm was used in the first experimental series, and a smaller Buchner funnel of diameter 6.2 cm was used in all the other series. The slot size of the funnels was 0.1 cm and the funnel had 91 slots.

-Next, the biomass was rinsed with water (40 °C) in the same equipment and collected from the top.

-The residual water of biomass was pressed out manually as effectively as possible.

-The washed biomass was dried in an oven or in air, milled and placed neatly for thermogravimetric analysis, TGA, to get representative, parallel samples.

The experimental parameters are listed in Table 11. The ash content and the biomass moisture content were measured with TGA. The size of the biomass sample in each test was 20 g.

A constant pure condensate-to-biomass mass ratio was 9:20 in the experimental series 1–2. This is the approximate maximum ratio in a fast pyrolysis plant based on the preliminary mass balance calculations. The condensate was then diluted with water to the amount indicated in Table 11.

In the seventh experimental series the previously defined optimal conditions for ash removal were utilized. The effect of the particle size of the biomass on the removal was studied. The chip size of the reference biomass was 0.55–0.92 mm, which is the same size used in the pilot scale experiments (see Chapter 4). The particle size of the biomass in the experimental series is presented in Chapter 3.3.

Table 11. Parameters of laboratory test series: biomass-washing liquid-slurry temperatures, T, residence times, t, biomass-to-washing liquid mass ratios and biomass-to-rinsing water mass ratios, biomass particle size, d_p. The colored cells show changed parameters.

Test no.	T [°C]	t [h]	Biomass-to-washing liquid mass ratio		Biomass-to-rinsing water mass ratio	d_p [mm]
			Cond.	HNO_3 (1 %)		
0	40	2	-	-	1:15	<5
1a	40	2	1:10	-	1:10	<5
1b	40	2	1:8	-	1:10	<5
1c	40	2	1:5	-	1:10	<5
2a	40	2	1:5	-	1:10	<5
2b	60	2	1:5	-	1:10	<5
2c	80	2	1:5	-	1:10	<5
3a	40	2	-	1:10	1:10	<5
3b	40	2	-	1:8	1:10	<5
3c	40	2	-	1:5	1:10	<5
4a	40	2	-	1:4	1:10	<5
4b	40	2	-	1:3	1:10	<5
4c	40	2	-	1:2	1:10	<5
5a	40	0.5	-	1:5	1:10	<5
5b	40	1	-	1:5	1:10	<5
5c	40	2	-	1:5	1:10	<5
6a	40	2	-	1:5	1:15	<5
6b	40	2	-	1:5	1:10	<5
6c	40	2	-	1:5	1:5	<5
7a	40	0.5	-	1:5	1:5	<5
7b	40	0.5	-	1:5	1:5	0.55–0.92

3.3 Experimental results

The experimental series 1–2 clarified the choice of the acidic liquid for the biomass alkali removal. The results of the series 1–2 were that the amount of the available condensate is insufficient and with this diluted washing liquid, adequate removal cannot be achieved even with higher temperatures. Consequently the rest of the experiments were carried out with nitric acid solutions, which had also given good results in previous studies (Stefanidis et al. 2015). The other aspects in selecting the acidic liquid are presented in Chapter 5.1.3.

The measurement error of temperature was evaluated to be ± 5 °C (Paasonen 2016), because the plate heaters were old and did not have an adjustable temperature sensor. The error of the ash removal efficiencies was estimated to be 5 % points. An example of this was that the ash removal efficiency was 39 % and 34 % in the experiment 1c and 2a, which had the same experimental conditions.

The experimental series 3–4 solved the optimal biomass-to-nitric acid solution mass ratio, which was 1:5. The ash removal efficiency was 54 %, when 100, 160 or 200 grams of 1 % nitric acid solution was used in the series 3. The ash removal efficiency was 48 %, when 80 g of 1 % nitric acid solution was used and 44 %, when 60 g or 40 g was used in the series 4.

In the experimental series 3, very large vacuum was used by accident, which caused bubble formation in the suction flask. Gases usually liberate at high temperatures and low pressures, so it was suspected that some gases, such as nitrogen oxides, were formed. The vacuum in the industrial rotary vacuum drum washer cannot be that large, because the pressures of the industrial rotary vacuum drum washers range between 10 – 85 kPa (see Chapter 2.4.1). Nonetheless, the vacuum has to be large enough, so that the rinsing will not drop the biomass from the surface of drum.

The optimal residence time was solved in the experimental series 5. The times of 0.5 h, 1 h and 2 h were tested. The ash removal was 49 %, when the residence time was 0.5 h or 1 h. The removal was not significantly higher, 54 %, with the time of 2 h. Consequently, the optimal residence time is 0.5 hours. The advantages of a shorter residence time are significant: the size of the tank, in which the slurry is created, is reduced, so the power consumption in mixing the slurry is noticeably reduced, and the price of the tank is also decreased.

In the experimental series 6, the optimal biomass-to-rinsing water mass ratio was defined. The ash removal efficiencies varied between 53–56 %, so the smallest mass ratio (1:5) was as good as the largest mass ratio (1:15) in the limitations of measurement accuracy.

Thermogravimetric analysis indicated that the average moisture content of the raw material was 38.8 % and the average ash content of raw material was 3.2 %. The ash removal efficiencies of the test series are presented in Table 12.

Table 12. Ash removal efficiencies of experimental series, η. Condensate is abbreviated as Cond. here. Concentration of HNO_3 was 1 %. Parameters are washing liquid, biomass-to-washing liquid mass ratio, w_{bs}, the biomass-washing liquid-slurry temperature, T, residence time, t, biomass-to-rinsing water mass ratio, w_{br}, and chip size, d_p. All parameters were optimal in experiment 7a.

	Variables						
Test no	Liquid	w_{bs}	T [°C]	t [h]	w_{br}	d_p [mm]	η [%]
0	Water	1:15					24
1a	Cond.	1:10					41
1b	Cond.	1:8					39
1c	Cond.	1:5					39
2a	Cond.		40				34
2b	Cond.		60				30
2c	Cond.		80				42
3a	HNO_3	1:10					54
3b	HNO_3	1:8					54
3c	HNO_3	1:5					54
4a	HNO_3	1:4					48
4b	HNO_3	1:3					44
4c	HNO_3	1:2					44
5a	HNO_3			0.5			49
5b	HNO_3			1			49
5c	HNO_3			2			54
6a	HNO_3				1:15		54
6b	HNO_3				1:10		56
6c	HNO_3				1:5		53
7a	HNO_3					< 5	50
7b	HNO_3					0.55–0.92	51

Particle size of biomass in the experimental series was determined using sieve series. Size distribution of biomass is presented in Figure 13 and visualized in Figure 14.

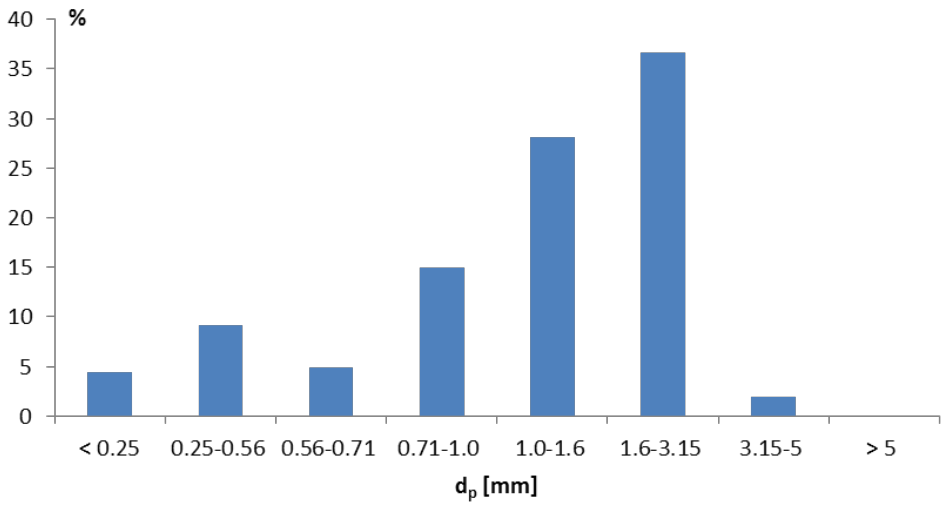

Figure 13. Particle size distribution of biomass in experimental series, d_p is diameter of particle.

Figure 14. Particle size scale of biomass in experimental series.

In the experimental series 7, the ash removal efficiency of the normal chip size biomass (see Figure 13) was compared to the smaller chip size biomass (0.55–0.92 mm). The result of the experimental series 7 was that the chip size of biomass hardly effected the ash removal. The ash removal efficiency for the larger particle size biomass was 50 % and for the smaller particle size biomass 51 %. The moisture content of the finer mass was 31 w-% and the moisture content of the coarser mass was 39 w-% in the beginning. Thus, the finer mass binds more liquid in the washing stage. The ash content of the finer biomass was 3.0 w-% and for the coarser biomass 3.2 in the beginning.

Concentrations of the AAEM ions and of some of their counter ions in the combined used washing liquid and rinsing water in the experiment 6a were measured by capillary electrophoresis, CE. The results of the CE are presented in Table 13. The detection limit of the method is <5 ppm. Table 13 shows that the total concentration of AAEMs in the used liquid was 480 ppm.

Table 13. Concentrations of AAEMs and of some of their counter ions in combined used washing liquid and rinsing water in experiment 6a

Ion	c [ppm]
Cl^-	<5
SO_4^{2-}	<5
HPO_4^{2-}	41
K^+	145
Ca^{2+}	202
Na^+	92
Mg^{2+}	40

$\sum \text{AAEMs} = 480$

3.4 Conclusions

According to these laboratory experiments, the optimal alkali removal process parameters were nitric acid as washing liquid, washing temperature 40 °C, residence time 0.5 h, biomass-to-washing liquid mass ratio 1:5, biomass-to-rinsing-water mass ratio 1:5 and the normal chip size (<5 mm). Rinsing water temperature was 40 °C and the nitric acid concentration 1 % in the experiments. These are the most important parameters affecting the alkali removal, although it should be noted that even more parameters might exist such as the salt concentration of the washing liquid. The goal for the removal (see Chapter 5.1.1) was achieved within the limitations of measurement accuracy. When the above-mentioned process conditions were used, the removal efficiency of biomass ash was 50 %. However, more extensive laboratory experiments on the washing of biomass are recommended, because the combined effects of different parameters were not explored in this thesis. Higher washing temperatures for the nitric acid wash should be investigated in the future.

4 Pilot scale experiment

4.1 Experimental plan

The purpose of the pilot scale experiment is to test the biomass alkali removal in a larger scale. Nitric acid solution is used for washing. The washed biomass is pyrolyzed, so that the increase of the organic liquid can be analyzed. This pilot scale experiment is a part of the Res2Heat –project at VTT.

4.2 Experimental setup

Approximately 10 kg (9.7 kg) forest residue biomass (particle size 0.55–0.92 mm) was washed with 50 kg nitric acid solution (1 %) and rinsed with tap water (40–50 kg). The slurry of biomass and washing liquid was kept in a tank for 30 minutes. The washing temperature was about 40 °C (43–44 °C). The slurry was mixed with a countercurrent mixer with the speed of 90 rpm. The mixer had four mixing elements on its axel and its blades a length of 37 cm. The motor of the mixer was SEW Eurodriven 1.1 kW electric motor and the manufacturer Uutechnic Oy. The mixer is presented in Figure 15. Thereafter, the biomass and the washing liquid were separated with a wire mesh sieve by pressing the liquid out manually. The wet cake was rinsed with water, after which the residual water was pressed out manually again. The temperature of the rinsing water was approximately 40 °C. The moisture and the ash contents of a sample of the cake were measured by TGA.

Figure 15. Uutechnic countercurrent mixer

At first, the pilot scale experiment was attempted to be carried out with a pressure filter (Outotec Larox), but the slurry was too viscose for it. The pump of the pressure filter got stuck immediately. This confirmed the choice of the equipment, the rotary vacuum drum washer for the plant scale.

The pyrolysis experiments were performed as follows (Lindfors 2016): The biomass used in the experiment was stored in a small gas-tight tank with the capacity of 4 kg. Raw material was fed into the pyrolysis from the feeding tank with a slowly rotating metering screw conveyor and a highly rotating feeding screw conveyor. The pyrolyzer was a bubbling fluidized bed reactor in nitrogen atmosphere. The pyrolysis temperature was 500 °C and the gas phase residence time 0.8 s. The char left after pyrolysis was separated from the gases with two cyclones. After the cyclones, hot vapours and gases were quenched rapidly into the liquid bio-oil product. Hot gases and vapours were cooled first with water indirectly in a stainless steel cooler after which an electrostatic precipitator was used to recover the aerosols from the gases. From the electrostatic precipitator the non-condensate and light organics were led to a glycol cooler where the vapours were cooled indirectly with cold glycol (5-10 °C). The glycol cooler is equipped with packings to capture the remaining liquid droplets from the gases.

After that, the gases were cooled to -50 °C step by step in a side stream sampler, not shown in Figure 16, to ensure nearly total recovery of residual water and light organics. The composition of the non-condensable gases was analysed by gas chromatography.

The schematic flow diagram of the bench scale fast pyrolysis unit (feed 1 kg/h) used in the experiments is shown in Figure 16 (Lindfors 2016).

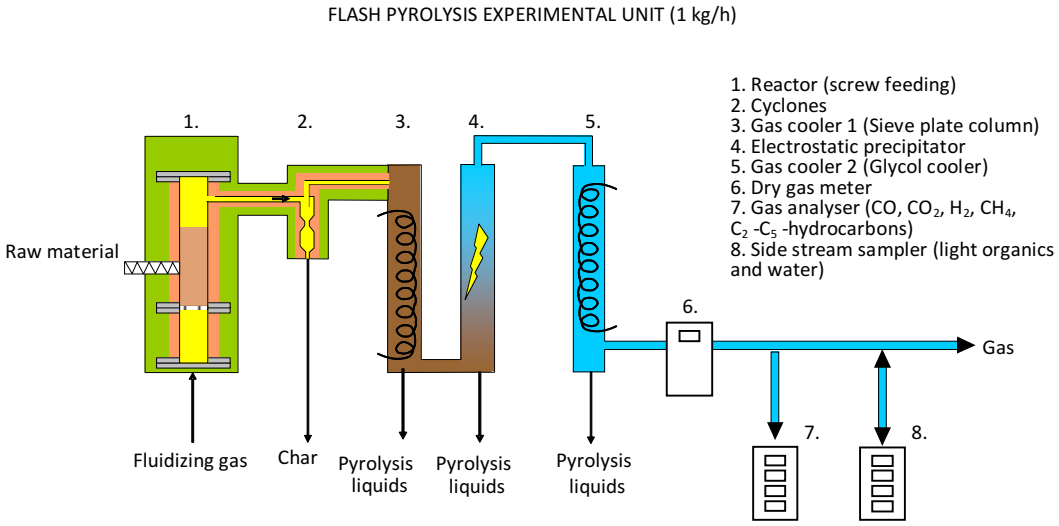

Figure 16. Schematic flow diagram of the bench scale fast pyrolysis unit at VTT

After the pyrolysis experiments, the collected char and bio-oil was weighed. Most of the organics in the bio-oil (≈95 w-%) were recovered in the stainless steel cooler and electrostatic precipitator (Figure 17). The product in the glycol cooler contained 60–80 w-% of water. The product after the glycol cooler was less than 5 % of the whole liquid. The liquid products in sieve plate column and electrostatic precipitator were mixed together before chemical characterization. The liquid from the glycol cooler was treated separately. Figure 17 presents the liquid products from the scrubber, electrostatic precipitator and glycol cooler. The liquid recovery system was rinsed after each experiment with a small amount of methanol to remove the condensed bio-oils from the walls of the condensers. The amount of pyrolysis liquid condensed on the walls was determined by evaporating methanol from the washing liquid with a rotavapor and weighing the residue. (Lindfors 2016)

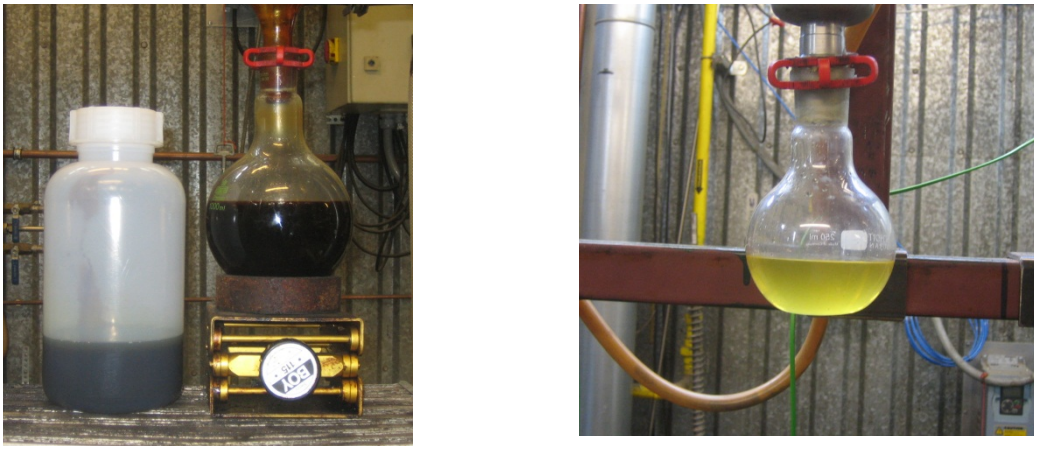

Figure 17. Liquid products from the scrubber, electrostatic precipitator (left) and glycol cooler (right).

4.3 Experimental results

The moisture content of the biomass was 32 % in the pilot scale experiment. The average moisture content in the laboratory experiments was instead about 39 % (see Chapter 3.3). The particle size in the pilot scale was 0.55–0.92 mm and in the laboratory scale <5 mm. It is actually <5 mm in the plant scale as well. The biomass had dried more in the crushing, when it was crushed into a smaller particle size. The biomass of a larger size will bind less liquid, so the slurry will be less viscous.

The moisture content of the biomass after pilot scale washing was 72 %, so the manual pressing was not very efficient. The ash content of the biomass in the beginning was 2.9 w-% and in the end 1.6 w-%, so the removal efficiency of ash was 45 %. The combination of the rotary vacuum drum washer and the mechanical press is expected to function better than this mostly manual system used. The reason for this is that the dissolved alkalis will be removed more efficiently, when more water is sucked and pressed out.

The treatment of the slurry will be easier in the plant scale in continuous operation than in this pilot scale experiment. In continuous operation, the slurry stays in motion to avoid the formation of deposit. The pipes are also wider. The outlet pipe could be placed to the bottom of the slurry-mixing tank, so that the cake formation in the bottom of the vessel will be minimized.

Based on this pilot scale experiment, it could be recommended to use more liquid to make the treatment of the slurry easier. Special attention has to be paid to the mixing and the pumping of the slurry. More experiments need to be done in the field.

The pyrolysis experiment revealed that the yield of organic liquid did not increase significantly, when 45 % of ash was removed, see Table 14. It presents the yields of the pyrolysis experiment on dry basis.

Table 14. Yields of pyrolysis experiment of forest residue on dry basis

Product	Unwashed [w-%]	Washed [w-%]
Organic liquid	53	56
Pyrolytic water	10	9
Pyrolytic gases	11	12
Cyclone char	23	21
Others	3	2

4.4 Conclusions

The biomass ash removal was 45 % in this pilot scale experiment. The removal was 51 % in laboratory, when the biomass had similar chip size. The combination of the rotary vacuum drum washer and the mechanical press in the plant scale is expected to function better than this mostly manual system used. The biomass-washing liquid slurry is rather viscose, so special attention has to be paid to its treatment such as mixing and pumping. However, the slurry will be less viscous in the plant scale, when the biomass of larger particle size will be used.

The pyrolysis experiment showed that the yield of the organic liquid was only slightly increased, when the washed biomass was used in pyrolysis instead of the regular forest residue. The yield was raised from 53 % to 56 % on dry basis.

5 Process design

5.1 Goal of removal

The goal of ash removal efficiency depends on several factors. Those are for example the requirements for the oil quality and the particulate emission limits in combustion. The bonding of ash compounds in the biomass also affects the goal of removal. The more ash is removed, the more resources such as liquid and energy are consumed. The goal of ash removal efficiency was set based on the production costs and the income of the improved quality of the new oil. Therefore only an approximate goal for the alkali removal efficiency is presented in this chapter.

The goal of the washing process is to reduce the ash content of the forest residue to the level of trunk tree (Oasmaa 2016). The mass percent of ash in trunk tree is w-% $_{\text{ash, trunk}}$, 0.60 %, on dry basis (Wilén et al. 1996). This goal is good enough for this case, because some of the ash compounds are organically bound to the structure of the biomass and thus cannot be removed by washing (see Chapter 2.3). Forest residue chips have the mass percent of ash, w-% $_{\text{ash, forest residue}}$, 1.3 on dry basis (Wilén et al. 1996). The goal for removal efficiency, Goal-%, is calculated according to Equation 14.

$$\text{Goal} - \% = \left(\frac{\text{w\% ash, forest residue} - \text{w\% ash, trunk}}{\text{w\% forest residue}}\right) \cdot 100\ \% \approx 54\ \% \qquad (14)$$

Hence, the goal of the process is to reduce the ash of the biomass 54 %. However, this is lower than the removal efficiencies previously described in literature, because relatively large amounts of liquid were used in those experiments (Stefanidis et al 2015).

5.2 Selection of acidic liquid

The selection of acidic liquid is based on its properties, efficiency of ash removal and price. The best options were nitric acid, hydrochloric acid and condensate. Sulfuric acid was considered also, but it was suspected to destroy the structure of biomass more than nitric acid and its waste liquid treatment is not easier, so it was not an alternative in this thesis (Solantausta 2016).

The condensate raised a lot of interest at first, since it is free waste flow of the existing process. Nevertheless, the laboratory tests (Chapter 3) revealed that the obstacle of the biomass wash with condensate is that the amount of condensate is small compared to the amount of the biomass in the plant. However, even a more serious problem of condensate wash would have been the complex waste liquid treatment after the process. The composition and properties of condensate from VTT's pilot centre are presented in Attachment 3. Attachment 3 shows that condensate contains toxic, corrosive, flammable and water-insoluble VOC-compounds (*Volatile organic compounds*), which should not be discharged to the drain as such (Joensuun vesi 2016). Placing the used condensate to the fluidized bed boiler would not have been an option either, because the vaporization of large flow rates of liquid would not have been feasible because of the large consumption of energy. Thus, if condensate was used in the alkali removal process, a waste water treatment plant should have been constructed, which would have raised the fixed capital investment. Therefore, there were two major reasons for rejecting the condensate as an alternative. Also the catalytic effect of ash can be passivated with the addition of small quantities of strong acids (Kuzhiyil et al 2012, Dalluge er al 2014), and since the condensate does not contain strong acids, another liquid was preferred.

Consequently, the choice of acidic liquid had to be made between nitric acid and hydrochloric acid. Unfortunately, the information of the propensity of hydrochloric acid to destroy the structure of biomass was not available, so it was not considered a safe choice for the removal. Nitric acid and hydrochloric acid

are both strong acids, so they protolyze completely. The acid constant, K_a [mol/dm^3] (25 °C), of nitric acid is 22 and for hydrochloric acid 10^7. (Taulukot.com 2016) Most of the published biomass washes had been performed with either condensate type liquid or dilute nitric acid (Oudenhoven 2013, 2015 and Stefanidis 2015), which supported our choice: the nitric acid. However, if hydrochloric acid would not destroy the structure of the biomass, it could be efficient in alkali removal thanks to its high acid constant. More research on this is required. Additionally, the product after neutralizing the hydrochloric acid with sodium hydroxide (sodium chloride) would be more environmentally friendly alternative than the product of nitric acid (sodium nitrate), because nitrates cause eutrophication. The properties of acidic liquids considered in this thesis are presented in Table 15. It shows that dilute nitric acid is solution of choice.

Table 15. Properties of acidic liquids

	Risk of structure destruction of biomass	Waste liquid treatment	Reverse osmosis of salts	Price [€/kg]	Other problems
Condensate	-	Difficult	No information	0	Small amount
HCl (dilute)	X	Complete neutralization possible	Excellent (e.g. NaCl 99 %)	0.135 €/kg (31 % HCl, Alibaba 2016c)	-
HNO_3 (dilute)	-	Complete neutralization possible	Very good (e.g. $NaNO_3$ 97%)	0.27 €/kg (68 % HNO_3, Alibaba 2016a)	-

Table 15 shows that the price of 68 % nitric acid is 0.27 €/kg (Alibaba 2016a). A similar price was also found elsewhere: 67 % nitric acid is 0.24 €/kg (Icis 2016).

5.3 Process principle

The flow chart of the alkali removal process is presented in Attachment 2.

The forest residue (moisture 40 %) is crushed into a finer particle size (to <5 mm). 40 °C 1 % nitric acid (1:5), is added to the tank, where the slurry is mixed for 30 minutes. The slurry is pumped to the rotary vacuum drum washer, in which the vacuum is applied so that the washing liquid gets out, and the cake stays on top of the drum. The filter cake is then rinsed with 40 °C water (1:5) in the same equipment, so the rinsing water and the washing liquid go to the same channel. The cake is discharged from the top of the drum and it is then pressed with a mechanical press to remove the residual water. The used acid is neutralized with sodium hydroxide solution according to Equation 15.

$$HNO_3 + NaOH \rightarrow NaNO_3 + H_2O \quad (15)$$

Water is recycled by reverse osmosis (see Chapter 2.4.2), which separates the salts. A small portion of the permeate flow and the retentate are led to the municipal waste water treatment plant. Alternatively, fertilizer could be manufactured from the waste water, see Chapter (6.1.7). The recycling permeate is divided into two flows, so that the inlet water consumption is divided more evenly between the two stages. The water from the pressing stage is also completely recycled to decrease the feed water need in the first stage.

5.4 Operating instructions

The operating instructions are based on the flow chart (see Attachment 2) and on the list of control instruments (see Attachment 6). These instructions are the preliminary guideline to be followed in the control room of the new unit.

The biomass is crushed in a crusher KA-1 and then conveyed with a screw conveyor JD-1. The biomass feed is controlled in the screw conveyor with the control instrument FFICA-1, which measures the flow rates 12 and 17.

Strong nitric acid (68 %) is stored in a tank FA-6, which is fulfilled every 14 days based on the tank sizing, see Chapter 6.2.3. Dilute nitric acid feed is formed in the vessel FA-1, where water and nitric acid are mixed with GD-1. Dilute nitric acid feed to process is controlled with FICA-1. The rinsing water feed is controlled with FICA-2. The water feed to FA-1 is controlled with instrument LICA-1. The nitric acid feed to FA-1 is adjusted with the instrument FFICA-2. The washing liquid is heated with heat exchanger EA-1 and the rinsing water is heated with heat exchanger EA-2.

The biomass and the washing liquid are mixed in the tank FA-4 with the mixer GD-3. The biomass-washing liquid slurry feed to GA-5 is adjusted with the control instrument LICA-2. The slurry is pumped with GA-5 to the container of the rotary vacuum drum washer (HA-1). The vacuum of the drum sucks the used washing liquid and rinsing water inside of the drum, as at the same time the biomass stays on top of the drum. The washed biomass is conveyed with the screw conveyor JD-2 to the mechanical press KE-1 and the pressed biomass is taken forward to the drying unit of the fast pyrolysis plant.

The used washing liquid is neutralized with sodium hydroxide. Sodium hydroxide is stored in tank FA-3, which is fulfilled every 14 days based on the tank sizing, see Chapter 6.2.3. Dilute sodium hydroxide feed is formed in the vessel FA-5, where water and strong sodium hydroxide are mixed with GD-3. Dilute sodium hydroxide feed is controlled with instrument FICA-3. The water feed to FA-5 is

controlled with LICA-3. Strong sodium hydroxide feed is controlled with the control instrument FFICA-3.

The salty water flow is pumped with GA-1 to the reverse osmosis unit HX-1. The reverse osmosis separates the salts, and permeate is led to FA-2. The flow rates 5, 6 and 14 are controlled with instrument LICA-4.

Pumps GA-2 and GA-3 raise the water approximately 20 meter, so that the water can be combined with the flows 13 and 9, respectively. Press water is recycled by pump GA-4. Rotating speeds of the screw conveyors are measured and controlled with instruments SIC-1 and SIC-2, the speed of HA-1 with instrument SIC-3 and the speeds of the mixers with instruments SIC-4, SIC-5 and SIC-6.

6 Techno-economic feasibility

6.1 Mass balances

6.1.1 Introduction

Three types of mass balances were calculated with Excel's Solver in this thesis: 1) the total balance, 2) the ash balance and 3) the sodium nitrate balance. The flow rates of nitric acid and sodium hydroxide, the mass concentrations of ash, nitric acid, sodium hydroxide and sodium nitrate, and pH were calculated also (see Attachment 1).

In chemical engineering, *steady state* is a situation, in which all state variables are constant. In this case, this means that outflow is equal to inflow. This can be applied also to individual components. So as long as the inflow of alkalis is as large as the outflow, the alkalis will not accumulate to the unit; instead they have a constant value inside the unit. The same applies to the total and sodium nitrate balances obviously. Since there are three recycles in the process, the steady state information is useful and applied in the calculation of the balances. The mass balance equations can be divided into two groups: the ones formed from the assumptions presented in this Chapter and the ones iterated with Excel's Solver. In the latter, all the variables are transformed to the left side of the equation and the right side is set to zero. Both of the balance equations types are obviously valid.

The assumptions of the balance calculations were as follows:

-The moisture content of the biomass is the same after the pressing as in the feed, 40 %. So the process does not increase the amount of water bound to biomass and thus the drying costs of the pyrolysis plant do not change. The usual moisture content after the pressing is 37–38 % (Wikberg 2016), when using the novel mechanical dewatering press invented by Stefan Sobota (see Chapter 2.4.3). According to Sobota, the moisture content of the biomass is even possible to reduce to the value of 29 % for example by using higher pressure (Sobota 2016). However, then the quality of the fiber may be slightly damaged.

-The mechanical press does not remove alkalis.

-The acid concentration after the water rinsing phase is close to zero.

-The $NaNO_3$ formed does not attach to biomass.

-The inner moisture of the raw material (~40 %) does not change into acid. This is a simplification, but the accuracy is good enough for this case (Melin 2016).

-The nitric acid and water will be fully mixed and the biomass binds them both in the relation that they are in the mixture. The salts are completely dissolved.

-The water permeability, p, of the reverse osmosis membrane is 75 % (see Chapter 6.2.6)

-Since the salt ions consist mostly of sodium nitrate, the ability of the membrane to separate this compound is most significant. The ash separation efficiency, r, for $NaNO_3$ is 97 % (Dow 2016a)

-When the total mass balance is calculated, the amount of the sodium nitrate and water formed in the neutralization reaction is small compared to the total amount of water

-The nitric acid is a strong acid and equimolar amount of it is used, so all of it reacts with sodium hydroxide to form sodium nitrate and water

-The biomass binds the liquid twice, when compared to its own mass, b = 2. Then the moisture content of the biomass after the rotary vacuum drum washer would be 70 %, when it actually is 86–90 % (Jussila 2016). However, the simplification was good enough in this case.

Based on the laboratory experiments, the following values were used in the calculations:

-Biomass-to-washing liquid mass ratio was 1:5.

-Biomass-to-rinsing water mass ratio was 1:5.

-The ash weight percent of the feed biomass ($w_{ash,feed} - \%$) was 3.2 % on average.

-The moisture content of the feed biomass was about 40 % on average.

-The weight percent of nitric acid was 1 %.

-The ash removal efficiency, η_{removal}, was 49 %.

-The residence time was 0.5 hours.

The limits in the balance calculations were as follows:

-The mass concentration of sodium hydroxide in FA-5, is 5 %

-Joensuun vesi can receive a waste water flow of 2000 m^3/d at the maximum (Kaukoranta 2016)

-The pH range of the reverse osmosis membranes is 2–7.

-The suitable amount of metals in washing liquid is 500 ppm (Baird et al. 2015)

- The pressure for reverse osmosis is 17–28 bars.

6.1.2 Total mass balance

Total mass balance was calculated with Equations 16–37. Equations 16–31 were calculated analytically, whereas Equations 32–37 were iterated with Solver. The flow rate 4 was calculated with Equation 16, flow rate 8 with Equation 17 and flow rate 10 with Equation 18. Equation 19 describes the neutralization reaction of nitric acid and sodium hydroxide and Equation 20 the balance of water recycling from the press. The flow rates of the washing liquid and the rinsing water were calculated from Equation 21. Equation 22 describes the second recycling. Equation 23 represents the mechanical press. Equation 24 describes the biomass flow rate to thermal drier. Equation 25 presents the mass balance of the tank FA-1, Equation 26 the tank FA-4, Equation 27 the tank FA-5 and Equation 28 the mass balance of the reverse osmosis.

Nitric acid and sodium hydroxide react completely, so their constant values in the cycles are 0. The flow rate of 68 % nitric acid was calculated from Equations 29–30 and the flow rate of 100 % sodium hydroxide from Equation 31. Equations 32, 33, 34, 35 and 36 describe the total balance, reverse osmosis, waste water treatment plant, first recycling and the drum, respectively. The flow rates calculated with Solver are $\dot{m}_1, \dot{m}_3, \dot{m}_5, \dot{m}_6, \dot{m}_7, \dot{m}_9$.

Flow $\dot{m}_6$ is the outflow of water from the tank FA-2. That flow was preferred to be rather small. Altogether, there was one variable in excess compared to the amount of the equations to be iterated. For these reasons, one more constraint was added to Solver according to Equation 37. This way, it was possible to solve all the equations.

$$\dot{m}_4 = (1 - p) \cdot \dot{m}_{11} \quad (16)$$

$$\dot{m}_8 = \dot{m}_2 \cdot b \quad (17)$$

$$\dot{m}_{10} = \frac{m_{100\ \%\ NaOH\ need}}{0.05} \quad (18)$$

$$\dot{m}_{11} = \dot{m}_3 + \dot{m}_{10} \quad (19)$$

$$\dot{m}_{13} = \dot{m}_1 + \dot{m}_{16} \quad (20)$$

$$\dot{m}_{12} = \dot{m}_{17} = 5 \cdot \dot{m}_2 \quad (21)$$

$$\dot{m}_{14} = \dot{m}_{12} - \dot{m}_9 \quad (22)$$

$$\dot{m}_{16} = \dot{m}_8 - \dot{m}_{15} \quad (23)$$

$$\dot{m}_{15} = \dot{m}_2 - \eta_{\text{removal}} \cdot w_{\text{ash,feed}} \cdot \dot{m}_2 \quad (24)$$

$$\dot{m}_1 = \dot{m}_{18} + \dot{m}_{19} \quad (25)$$

$$\dot{m}_2 + \dot{m}_{17} = \dot{m}_{20} \quad (26)$$

$$\dot{m}_{10} = \dot{m}_{21} + \dot{m}_{22} \quad (27)$$

$$\dot{m}_{11} = \dot{m}_4 + \dot{m}_{23} \quad (28)$$

$$\dot{m}_{18} = \frac{0.01 \cdot \dot{m}_{17}}{0.68} = \dot{m}_{HNO_3,1} \quad (29)$$

$$\dot{m}_{HNO_3,1} = \dot{m}_{HNO_3,3} = \dot{m}_{HNO_3,13} = \dot{m}_{HNO_3,17} \quad (30)$$

$$\dot{m}_{21} = \frac{\left(\frac{0.68 \cdot \dot{m}_{HNO_3,3} \cdot 1000}{M_{HNO_3}}\right) \cdot M_{NaOH}}{1000} = \dot{m}_{NaOH,10} \quad (31)$$

$$\dot{m}_1 + \dot{m}_2 + \dot{m}_9 + \dot{m}_{10} - \dot{m}_7 - \dot{m}_{15} = 0 \quad (32)$$

$$\dot{m}_4 + \dot{m}_5 + \dot{m}_6 + \dot{m}_{14} - \dot{m}_{11} = 0 \quad (33)$$

$$\dot{m}_4 + \dot{m}_6 - \dot{m}_7 = 0 \quad (34)$$

$$\dot{m}_5 + \dot{m}_{13} - \dot{m}_{17} = 0 \quad (35)$$

$$\dot{m}_2 + \dot{m}_{12} + \dot{m}_{17} - \dot{m}_3 - \dot{m}_8 = 0 \quad (36)$$

$$0.2 \frac{kg}{s} \leq \dot{m}_6 \leq 0.3 \frac{kg}{s} \quad (37)$$

6.1.3 Ash balance

The alkalis in the system originate only from the biomass. There are two outflows of alkalis: the flow to the waste water treatment plant and the flow to the biomass thermal dryer.

The ash balance was calculated with Equations 38–49. Equations 38–47 were solved analytically, whereas Equations 48–49 were iterated with Solver. Equation 38 presents the flow rate 4 of ash with the rejection value of the membrane. The permeate flow rate of ash was divided into the three flows $\dot{m}_{ash,5}$, $\dot{m}_{ash,6}$ and $\dot{m}_{ash,14}$ according to Equations 39–41. Equation 42 presents the flow rate of ash to the waste water treatment plant and Equation 43 to the drying unit. Equation 44 describes the flow rate of ash in the rinsing phase, Equation 45 in the washing stage, Equation 46 in the slurry-tank and Equation 47 in the permeate. Equation 48 describes the drum and Equation 49 represents the total balance of ash. The flow rates of ash, $\dot{m}_{ash,3}$ and $\dot{m}_{ash,15}$, were calculated with Solver.

$$\dot{m}_{ash,4} = r \cdot \dot{m}_{ash,11} \quad (38)$$

$$\dot{m}_{ash,5} = \frac{\dot{m}_5}{\dot{m}_5+\dot{m}_6+\dot{m}_{14}} \cdot \left(\dot{m}_{ash,11} - \dot{m}_{ash,4}\right) \quad (39)$$

$$\dot{m}_{ash,6} = \frac{\dot{m}_6}{\dot{m}_5+\dot{m}_6+\dot{m}_{14}} \cdot \left(\dot{m}_{ash,11} - \dot{m}_{ash,4}\right) \quad (40)$$

$$\dot{m}_{ash,14} = \frac{\dot{m}_{14}}{\dot{m}_5+\dot{m}_6+\dot{m}_{14}} \cdot \left(\dot{m}_{ash,11} - \dot{m}_{ash,4}\right) \quad (41)$$

$$\dot{m}_{ash,7} = \dot{m}_{ash,4} + \dot{m}_{ash,6} \quad (42)$$

$$\dot{m}_{ash,8} = \dot{m}_{ash,15} \quad (43)$$

$$\dot{m}_{ash,12} = \dot{m}_{ash,14} \quad (44)$$

$$\dot{m}_{ash,17} = \dot{m}_{ash,5} \quad (45)$$

$$\dot{m}_{ash,2} + \dot{m}_{ash,17} = \dot{m}_{ash,20} \quad (46)$$

$$\dot{m}_{ash,5} + \dot{m}_{ash,6} + \dot{m}_{ash,14} = \dot{m}_{ash,23} \quad (47)$$

$$\eta \cdot \dot{m}_{ash,2} + \dot{m}_{ash,17} + \dot{m}_{ash,12} - \dot{m}_{ash,3} = 0 \quad (48)$$

$$\dot{m}_{ash,2} - \dot{m}_{ash,15} - \dot{m}_{ash,7} = 0 \quad (49)$$

6.1.4 Sodium nitrate balance

Sodium nitrate mass balance was calculated with Equations 50–60. Equations 50–57 were solved analytically, whereas Equations 58 and 59 were iterated with Solver and Equation 60 was placed in Equation 59. Equation 50 describes the flow rate 4 of sodium nitrate with the rejection of the membrane. The permeate flow of sodium nitrate was divided into the three flows $\dot{m}_{NaNO_3,5}$, $\dot{m}_{NaNO_3,6}$ and $\dot{m}_{NaNO_3,14}$ according to Equations 51–53. The flow rate of sodium nitrate to the waste water treatment plant was calculated with the Equation 54. Equation 55 presents the flow rate of sodium nitrate in the rinsing phase and Equation 56 in the washing stage. Equation 57 describes the permeate flow rate of sodium nitrate. Equation 58 represents the mass balance of the drum and Equation 59 the balance of the sodium nitrate forming. The sodium nitrate flows, $\dot{m}_{NaNO_3,3}$ and $\dot{m}_{NaNO_3,11}$, were calculated with Solver. The Solver is presented in Figure 18. Figure 18 shows that one of the equations to be iterated is set as objective, and it has the value of zero. Other equations to be iterated were defined as zero by adding constraints.

$$\dot{m}_{NaNO_3,4} = r \cdot \dot{m}_{NaNO_3,11} \quad (50)$$

$$\dot{m}_{NaNO_3,5} = \frac{\dot{m}_5}{\dot{m}_5+\dot{m}_6+\dot{m}_{14}} \cdot \left(\dot{m}_{NaNO_3,11} - \dot{m}_{NaNO_3,4}\right) \quad (51)$$

$$\dot{m}_{NaNO_3,6} = \frac{\dot{m}_6}{\dot{m}_5+\dot{m}_6+\dot{m}_{14}} \cdot \left(\dot{m}_{NaNO_3,11} - \dot{m}_{NaNO_3,4}\right) \quad (52)$$

$$\dot{m}_{NaNO_3,14} = \frac{\dot{m}_{14}}{\dot{m}_5+\dot{m}_6+\dot{m}_{14}} \cdot \left(\dot{m}_{NaNO_3,11} - \dot{m}_{NaNO_3,4}\right) \quad (53)$$

$$\dot{m}_{NaNO_3,7} = \dot{m}_{NaNO_3,4} + \dot{m}_{NaNO_3,6} \quad (54)$$

$$\dot{m}_{NaNO_3,12} = \dot{m}_{NaNO_3,14} \quad (55)$$

$$\dot{m}_{NaNO_3,5} = \dot{m}_{NaNO_3,17} = \dot{m}_{NaNO_3,20} \quad (56)$$

$$\dot{m}_{NaNO_3,23} = \dot{m}_{NaNO_3,11} - \dot{m}_{NaNO_3,4} \quad (57)$$

$$\dot{m}_{NaNO_3,12} + \dot{m}_{NaNO_3,17} - \dot{m}_{NaNO_3,3} = 0 \quad (58)$$

$$\dot{m}_{NaNO_3,3} + \dot{m}_{NaNO_3 formed} - \dot{m}_{NaNO_3 11} = 0 \quad (59)$$

In which

$$\dot{m}_{NaNO_3 formed} = \frac{\left(\frac{0.68 \cdot \dot{m}_{HNO_3,3} \cdot 1000}{M_{HNO_3}}\right) \cdot M_{NaNO_3}}{1000} \quad (60)$$

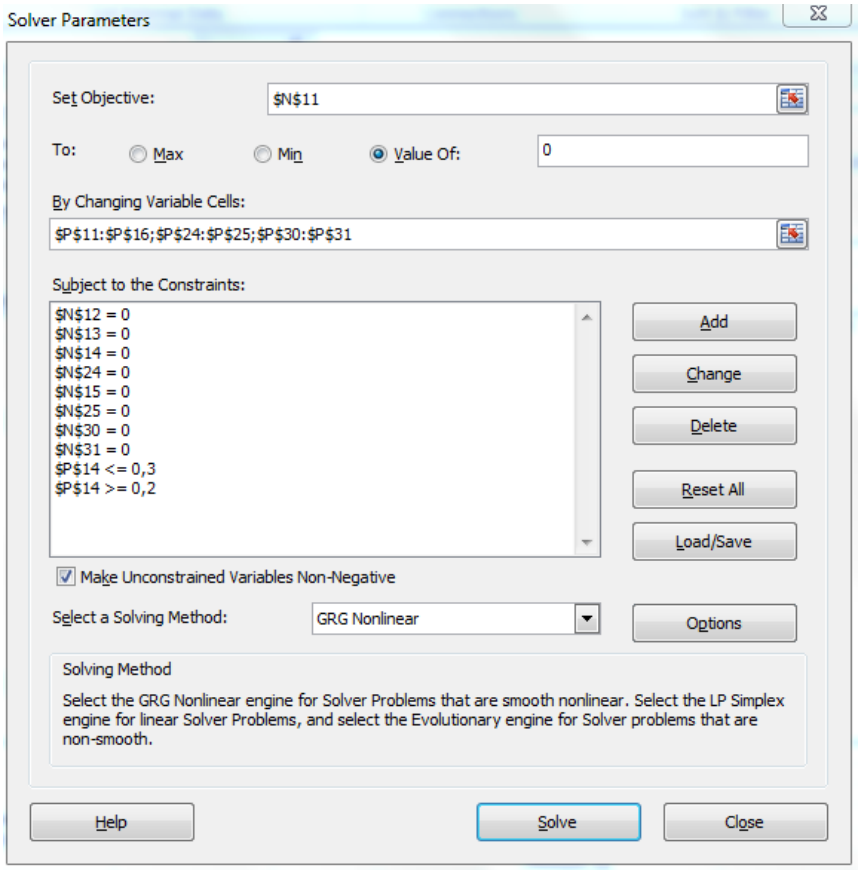

Figure 18. Solver in mass balance calculations.

6.1.5 pH

Since nitric acid is strong acid, it becomes protolyzed completely, which is demonstrated in Equations 61–62. When the volume is constant, also the concentrations of these components are equal. The pH of the nitric acid containing flows was then calculated from Equation 63. The concentration of nitric acid was calculated from Equation 64. The pH of the flows containing just water and salts is obviously 7. The pH of the sodium hydroxide containing flows was calculated according to Equations 67–69. Sodium hydroxide is strong base, so it also becomes protolyzed completely.

$$HNO_3 + H_2O \rightarrow NO_3^- + H_3O^+ \quad (61)$$

$$n(HNO_3) = n(H_3O^+) \quad (62)$$

$$pH = -\log[H_3O^+] = -\log[HNO_3] \quad (63)$$

$$[HNO_3] = \frac{\dot{n}(HNO_3)}{\dot{V}_i} \quad (64)$$

In which

$$\dot{n}(HNO_3) = \left(\frac{0.68 \cdot \dot{m}_{HNO_3 68\%,3} \cdot 1000}{M_{HNO_3}}\right) \quad (65)$$

$$\dot{V}_i = \frac{\dot{m}_i}{\rho_{H_2O} \cdot w_{H_2O} + \rho_{HNO_3} \cdot w_{HNO_3}} \quad (66)$$

$$pOH = -\log[OH^-] = -\log[NaOH] \quad (67)$$

$$pH = 14 - pOH \quad (68)$$

$$[NaOH] = \frac{\dot{n}_{NaOH}}{\dot{V}_i} \quad (69)$$

In which

$$\dot{n}_{NaOH} = \dot{n}(HNO_3) = \frac{0.68 \cdot \dot{m}_{HNO_3 68\%,3} \cdot 1000}{M_{HNO_3}} \quad (70)$$

$$\dot{V}_i = \frac{\dot{m}_i}{\rho_{H_2O} \cdot w_{H_2O} + \rho_{NaOH} \cdot w_{NaOH}} \quad (71)$$

The flow 3 has pH <2 (see Attachment 1), which is why it is neutralized before reverse osmosis.

6.1.6 Conclusion

All the flow rates, mass concentrations and pH calculated from the mass balances are presented in Attachment 1. The mass balances are utilized also in the variable cost calculations (see Chapter 7.2.2).

The only waste flow of the process can be led to the municipal waste water treatment plant, since it consists of just water, sodium nitrate (2.8 %) and other ash compounds (0.6 %). The environmental permit for this should be applied anyway. There is a possibility of manufacturing fertilizer from sodium nitrate and other ash compounds with reverse osmosis and vaporization of water. 97 % of sodium nitrate can be separated from water with reverse osmosis (Dow 2016a). The flow rate of sodium nitrate is about 300 g/s in the unit (see Attachment 1) and the market price of sodium nitrate (99.3 %) is 0.41–0.45 €/kg (Alibaba 2016d), so this alternative could be studied further. If the fertilizer was used in the surrounding area of the plant, there would not even be particular restrictions on the water content of the fertilizer, and the vaporization of water may not be even required.

The calculated values were compared to the limits (see Chapter 6.1.1). The flow rate of waste water is 977 m^3/d. This is expected to be appropriate flow for municipal waste water treatment in Joensuu. Table 16 shows that the mass concentration of the sodium nitrate formed or the other ash compounds in the washing liquid or in the rinsing water is not a problem. Table 16 shows also that the amounts of sodium nitrate and other ash compounds are slightly larger in the rinsing water than in the washing liquid. This is due to the fact that the alkali-free press water is recycled to the first stage. Sodium nitrate share of ash in the flow 11 is over 81 %. The salt percent of total flow 11 is 0.89 %. So the assumptions for the reverse osmosis were all right as well.

Table 16. Mass concentrations of sodium nitrate formed and other ash compounds in washing liquid and rinsing water.

Flow no	Description	$NaNO_3$ [ppm]	Ash [ppm]
17	Washing liquid	160	40
12	Rinsing water	260	60

6.2 Sizing and pricing of equipment

6.2.1 Introduction

The method for sizing and pricing of equipment depends on the individual piece of equipment used. However, many similarities in sizing and pricing principles exist. Sizing is usually based on flow rates, the capacities of equipment, residence times and the shapes of equipment. The sizing of heat exchangers is based on the desired temperature difference also. Pricing is usually based on the sizes of equipment and materials chosen. The pricing of pumps is based on head of pump or pressure difference desired.

The equipment for the flows of relatively low pH-values should tolerate corrosion. Corrosion resistant materials for dilute nitric acid solution include stainless steel 304 and 316, Hastelloy C276, titanium and some plastics such as epoxy, polypropylene and polytetrafluoroethylene, PTFE. However, alkali and alkaline earth metals are incompatible with plastics, and titanium and hastelloy are more expensive than stainless steel, hence the construction material of most equipment is stainless steel, SS 304 or SS 316. (Hurme 2008) However, when the flow consists of just water and salts, carbon steel, CS, can be used.

In this thesis, the equipment price estimates are based on as current information as possible. The prices were inquired from the manufacturers, sought from their

websites, taken from correlations in literature or from the Process Design Manual (Hurme 2008). Once a 20-year old correlation was used, but it was updated by multiplying with the inflation factor. However, due to the economic recession of past years, the inflation has not been so large, so this also helps us to get as valid pricing data as possible. The dollars were converted to euros by multiplying them with the factor 0.9, which was the dollar exchange rate to euros at the moment of the calculations.

6.2.2 Rotary vacuum drum washer

The rotary vacuum drum washer, HA-1, was sized based on its capacity. The daily capacity of the rotary vacuum drum washer is 8 t/m^2 softwood and 6 t/m^2 hardwood (Tarleton et al. 2007). The fast pyrolysis raw material is Finnish forest residue, which consists of about 85 % softwood and 15 % hardwood (see Chapter 2.2). Consequently, the capacity, c, of the rotary vacuum drum washer was calculated according to Equation 72.

$$c = 0.85 \cdot 8 \frac{t}{m^2 \cdot d} + 0.15 \cdot 6 \frac{t}{m^2 \cdot d} = 7.7 \frac{t}{m^2 \cdot d} \quad (72)$$

The mass transfer is assumed to occur only in the jacket of the cylinder. The feed flow rate of the biomass is 400 tons/day, so the area, A, of the desired wire mesh jacket of the cylinder is 52 m^2.

The radius, diameter, length and volume of the rotary vacuum drum washer were calculated also. The rotary vacuum drum washer has the shape of a cylinder, so its measures are calculated from Equation 73. The length of the drum is expected to be six times as high as its radius.

$$V = \frac{3}{4} \pi d^3 \quad (73)$$

In which V = volume, d = diameter

The rotary vacuum drum washers for these measures are available. For example, GL&V manufactures them in standard diameters: 2.44 m, 2.90 m, 3.51 m and 4.11 m and lengths range between 2.44–9.14 m (GL&V 2014). In this case, the purchase price of the rotary vacuum drum washer is evaluated to be 1 100 000 € (Jussila 2016). The sizing and pricing of the rotary vacuum drum washer is presented in Table 17, in which the radius, diameter, volume, length, rotating speed, power and cost are presented. The material of the rotary vacuum drum washer is stainless steel 304. The power consumption is approximately 37.5 kW (Jussila 2016). The generation of the vacuum for the rotary vacuum drum washer does not need a motor, so it was not taken into account in calculating electricity. The vacuum is formed with a squeegee. The moisture content of the biomass after the rotary vacuum drum washer is 86–90 % (Jussila 2016). The typical rotation speed of rotary vacuum drum washer is 5 rpm (Biermann 1996).

Table 17. Parameters of rotary vacuum drum washer.

Name	A_{jacket} [m^2]	r [m]	d [m]	V [m^3]	l [m]	s [rpm]	P [kW]	C [k€]
HA-1	52	1.2	2.3	31	7.0	5	37.5	1100

6.2.3 Tanks

There are six tanks in this process: FA-1, FA-2, FA-3, FA-4, FA-5 and FA-6. The tanks were sized based on the flow rates. The tanks were designed not to be more than 90 % full (Hurme 2008). The tanks FA-1, FA-2 and FA-5 were designed to have the capacity to store the process flow of ten minutes, so that the pumping is easy and there will be enough time to mix the HNO_3 and water as well as NaOH and water. The sizes of the raw material storage tanks are often selected for 30 days need (Hurme 2008). However, the capacity of the storage

tanks was designed for 14 days requirement, because HNO_3 and NaOH are easily available chemicals and they can be purchased in smaller batches. For example, the minimum order quantity of nitric acid by Alibaba is 20 tons (Alibaba 2016a). Minimizing the sizes of the storage tanks for hazardous chemicals is also one important principle of inherent safety.

The heights of the tanks are designed to be three times as large as the diameters. The tanks have the shapes of a cylinder, so the mathematical formula of a cylinder (see Chapter 6.2.2) was utilized in the sizing calculations. The heights, diameters and volumes of the tanks are listed in Table 18. The purchase prices of the tanks were estimated according to their volumes from the graph in Process Design Manual in page 107 (Hurme 2008). These prices were multiplied by the material factors presented in Table 18. It indicates that all the tanks are stainless steel (SS), except tank FA-2, which is carbon steel (CS), because it contains only water and salts.

Table 18. Tank dimensions, materials and costs

	Measures			Material		
Name	d [m]	h [m]	V [m^3]	Quality	Factor	C [k€]
FA-1	1.2	3.5	3.8	SS 316	2.1	6.9
FA-2	2.2	6.5	24	CS	1.0	7.4
FA-3	3.4	10.2	92	SS 304	2.4	56.4
FA-4	3.1	9.3	69	SS 304	2.4	42.0
FA-5	0.9	2.8	2.0	SS 304	1,7	4.1
FA-6	5.0	15.1	302	SS 316	2,7	202.5

6.2.4 Pumps

There are 10 pumps in the process area: GA-1A, GA-2A, GA-3A, GA-4A, GA-5A plus GA-1B, GA-2B, GA-3B, GA-4B and GA-5B. The five first mentioned are actively in use and the five latter are spare pumps. The pumps can be categorized into three different types: pumps for the raising of liquid (GA-2A/B, GA-3A/B, GA-4A/B), reverse osmosis feed pumps (GA-1A/B) and slurry feed pumps (GA-5A/B). Thus, every pump type has its own function, which is either 1) raising the potential energy 2) raising the pressure or 3) transporting the viscous slurry.

All the pumps for the raising of liquid are centrifugal pumps in this process. The important advantages of centrifugal pumps include simplicity, low investment and operating costs, uniform flow and small size. (Steele 2015)

The power consumption of pumps generally depends on the pressure difference desired, head, density, volume flow and pump efficiency. The power, P_E, can be calculated from Equation 74.

$$P_E = \frac{\Delta p \cdot V}{\eta} = \frac{\rho g h \cdot V}{\eta} \quad (74)$$

In which Δp = pressure difference, V = volumetric flow, η = pump efficiency, ρ = density, g = gravitational acceleration, h = head

The details of the centrifugal pumps and the reverse osmosis feed pumps were inquired from Sulzer Pump Finland. The pumps for the raising of liquid can be for example Sulzer SNS End Suction Single Stage Centrifugal Pumps and the feed pumps for the reverse osmosis Sulzer MBN Multistage Ring Section Pumps. The estimates for the purchase prices of the pumps are: GA-1 is 44 k€, GA-2 4.2 k€,

GA-3 4.7 k€ and GA-4 3.7 k€. The efficiency for all these pumps is 0.7. The estimations of the power consumptions are: GA-1 uses 160 kW, GA-2 7.5 kW, GA-3 11 kW and GA-4 2.2 kW. (Heikkilä 2016) The feed pumps for the reverse osmosis should achieve the pressure difference of 22.5 bars on average (Bradshaw 1997). Own evaluation for the heads of GA-2A/B and GA-3A/B was 20 meters and GA-4A/B 10 meters.

In this process, the feed pumps of the slurry are Bredel hose pumps, which endure acidic conditions and suit for continuous pumping of high viscosity fluids. Bredel 2100 has the largest capacity of the Bredel hose pumps available, which is 108 m^3/h at the maximum. (Watson-Marlow 2016) The budget price of one Bredel 2100 pump is 48 k€ and the power consumption per pump is 37 kW (Partanen 2016). The slurry feed is 110 m^3/h; therefore, the purchase prices and energy consumptions, were updated with a capacity exponent (Hurme 2008). This is presented in Equations 75–76. The typical value of the capacity exponent is 0.7 (Melin 2016).

$$C_{new} = C_{old} \cdot \left(\frac{c_{new}}{c_{old}}\right)^{k} \quad (75)$$

$$P_{new} = P_{old} \cdot \left(\frac{c_{new}}{c_{old}}\right)^{k} \quad (76)$$

In which C = cost, c = capacity, k = capacity exponent, P = power

The technical values related to the pumps of the process are presented in Table 19.

Table 19. Pump details

Name	ṁ [kg/s]	ρ [kg/l]	pH	H [m]	Δp [bar]	P [kW]	C/piece [k€]
GA-1A/B	44	1.0	7	-	22.5	160	44
GA-2A/B	13	1.0	7	20	-	7.5	4.2
GA-3A/B	20	1.0	7	20	-	11	4.7
GA-4A/B	4.7	1.0	7	10	-	2.2	3.7
GA-5A/B	28	0.9	0.9	-	-	38	49

6.2.5 Screw conveyors

There are two screw conveyors in the process, JD-1 and JD-2. JD-1 conveys the crushed biomass to the mixing tank of slurry and JD-2 transports the washed biomass to the mechanical press. The pressed biomass can be carried to the drying unit with an existing conveyor. The length of JD-1 was estimated to be 4 meters and JD-2 6 meters. In this process, the screw conveyors drive the biomass horizontally, so they can be at least 45 % full. Their diameters and maximum recommended speeds were designed according to their capacities, which were figured out by the flow rates. (Walas 2012) The power consumption of the screw conveyor can be calculated from Equation 77 (Sinnott 2013).

$$\mathrm{P} = 0.028 + 0.0139\mathrm{ml}^{0.8} \qquad (77)$$

Where P = power consumption [kW], m = mass flow [t/h] and $\mathrm{l} =$ conveying distance [m]

Prices of the screw conveyors were estimated based on their lengths (Page 1996). The prices were 2.1 k€ for JD-1 and 2.3 k€ for JD-2. However, there prices were from the year 1996, so they were updated to 2016 by multiplying them

with the inflation factor (1.37), which was applied from the web page of the Bank of Finland Museum (Anonymous 2016). All the sizing and pricing information of the screw conveyors is presented in Table 20.

Table 20. Details of screw conveyors.

Name	l [m]	P [kW]	s [rpm]	d [m]	C [k€]
JD-1	4	0.7	140	0.3	2.8
JD-2	6	2.0	140	0.3	3.1

6.2.6 Reverse osmosis

The sizing of the reverse osmosis unit, HX-1, was based on the volumetric flow of the permeate. The feed water of the reverse osmosis contains less than 0.9 % of salts, so it can be classified as brackish water (see Chapter 2.4.2). Industrial RO systems can typically recover 50–85 % of water depending on the feed water characteristics for example (Puretec 2016). The recovery values are higher for brackish water than sea water. Therefore, an own estimation of the recovery value of 75 % was used.

The number of RO elements in a system can be calculated with Equation 78 (Puretec 2016).

$$\text{No of RO elements} = \frac{\dot{V}_{\text{permeate}}\left(\frac{\text{m}^3}{\text{s}}\right)}{\varphi \cdot \text{A}} \qquad (78)$$

In which $\dot{V}_{\text{permeate}} =$ permeate flow rate, $\varphi =$ flux $\left(\frac{\text{m}^3}{\text{m}^2 \cdot \text{s}}\right)$ and $A_1 =$ area of one element (m^2)

The type of membrane in the RO system was selected to be Dow Filmtec BW30-365. Consequently, the area of each element is 34 m^2. (Dow 2016b) A typical brackish water flux is 0.0000066 $\frac{m^3}{m^2 \cdot s}$ (Puretec 2016). Thus, the number of elements was calculated to be 148. The price of reverse osmosis membrane is 13.13–17.75 €/m^2 (Jacob 2016), so the average, 15.44 €/m^2, was used here for the calculation of the purchase price. The sizing and pricing of RO are presented in Table 21, in which the permeate flow rate, flux, water permeability, active area/element, number of elements, membrane price and the total cost of reverse osmosis membranes are presented.

Table 21. Details of reverse osmosis unit.

Name	$\dot{V}_{perm.}$ [m^3/s]	φ $\left[\frac{m^3}{m^2 \cdot s}\right]$	p [%]	A_1 [m^2]	No. of elements	C_m [€/m^2]	$C_{RO\ total}$ [k€]
HX-1	0.033	0.0000066	75	34	148	15.4	77.6

6.2.7 Mixers

There are three tanks, which require mixing in the unit. The mixers are named GD-1, GD-2 and GD-3. The tanks to be mixed are FA-1, FA-5 and FA-4. The two first-mentioned contain liquids and the latter slurry. The type of GD-1 and GD-2 is pitched blade turbine, which was selected because it provides both radial and axial flow (Fusion Express 2016).

Fusion Express is a U.S. manufacturer of mixers. The prices for the mixers GD-1 and GD-2 were taken from their catalog. The standard material for the pitched blade mixers is stainless steel 316. (Fusion Express 2016) The mixing of the tanks FA-1 and FA-5 is simple, because they contain only liquids and have small sizes (see Table 22). Liquid-liquid-mixing power consumption is typically 1 kW/m^3

(Hurme 2008). The diameters of the mixers GD-1 and GD-2 were evaluated to be 1/3 of the diameter of the tank to be mixed.

The mixing tank for the slurry has a rather large size, 69 m^3 and demanding material to be mixed. Usually, the largest volume of a tank that can be mixed normally is about 40 m^3. Larger tanks should have the mixer on the side of the tank. (Vuori 2016) However, in this case the mixing on the side of a tank was not an option, because it does not work for the viscous slurry. The diameter of such mixer is not large enough to get the entire slurry moving. The recommended mixing system from Uutechnic Oy has four hydrofoil propellers as the mixing elements. The propellers have diameters of 2.8 meters and rotating speeds of 23 rpm. The system has the power consumption of 22 kW and the price of 42.4 k€. (Laine 2016) The technical values related to the mixers are presented in Table 22. Those are tank sizes to be mixed, densities of material to be mixed, lengths of the impellers, power consumptions, rotating speeds and costs.

Table 22. Technical values related to mixers.

Name	Tank	Content	V_{Tank} [m^3]	ρ [kg/m^3]	$l_{impeller}$ [m]	P [kW]	C [k€]
GD-1	FA-1	Liquid	3.8	1.0	0.4	3.4	0.51
GD-2	FA-5	Liquid	2.0	1.1	0.2	1.8	0.25
GD-3	FA-4	Slurry	69	0.9	2.8	22	42.4

6.2.8 Heat exchangers

The wash liquid and rinsing water are heated to 40 °C with the heat exchangers EA-1 and EA-2, respectively. They use district heating return water, which has the constant temperature of 60 °C (Solantausta 2016). EA-1 and EA-2 are similar heat exchangers, made of stainless steel 316.

The cold flow warms up from 10 °C to 40 °C. The hot flow cools down from 60 °C to 40 °C. Countercurrently operating plate heat exchanger was selected as the type, because it is commonly used and small. The overall heat transfer coefficient for this situation is 1700 W/m^{2}K (Engineering Tool Box 2016b). The prices were taken from a graph based on the areas of the heat exchangers (Loh 2002). The technical values related to the heat exchangers are presented in Table 23. Those are flow rate of district heating return water, logarithmic mean temperature difference, overall heat transfer coefficient, area per one heat exchanger and cost.

Table 23. Technical values related to heat exchangers EA-1 and EA-2.

Name	$\dot{m}_h$ [t/h]	ΔT_{LM} [°C]	U [W/m^{2}K]	A_{EA} [m^2]	C [k€]
EA-1, EA-2	124	24.7	1700	68.9	32.4

6.2.9 Mechanical press

The novel mechanical dewatering press, presented in Chapter 2.4.3, is available for the biomass and water separation. Etteplan manufactures those to the individual requirement of each customer (Sobota 2016). However, at the moment that equipment is used only in the laboratory scale and one pilot project (Thelander 2016). The details of the press in this case were inquired straight from the inventor, Stefan Sobota. In this situation, the moisture content of the

biomass after pressing is 40 w-% (see Chapter 6.1.1) and the flow rate to the press is 33.1 t/h (47.3 m^3/h). The purchase price for the press was evaluated to be 300 000 € and the energy consumption 100–160 kWh, so an average, 130 kWh, was used here (Sobota 2016). Table 24 presents the details of mechanical press.

Table 24. Technical details of mechanical dewatering press.

Name	$\dot{V}_8$[m^3/h]	w_{moist} [w-%]	E [kWh]	C [k€]
KE-1	47.3	40	130	300

6.2.10 Crusher

Proper crushing before washing is important, so that the washing liquid has enough contact area with biomass, and the removal of alkalis will be efficient. The desired crusher (KA-1) already exists in the Joensuu fast pyrolysis plant, where it is referred to as “the fine milling unit”. The crusher is a cutting and fast-functioning Kamas crusher. The moisture of the material is not harmful for the crusher. (Ratinen 2016) This crusher will be relocated from its original place after the drying unit to the new place before the alkali removal unit in connection with a conventional (summer) shutdown of the plant. The capacity of the press may decrease, when the biomass has more moisture. This aspect is not yet considered in this thesis.

The energy consumption of crushing depends on the desired chip size according to Equation 79 (Ratinen 2016). Some examples of the energy consumption of crushing are presented in Table 25. Based on the laboratory experiments, the

conventional chip size (<5 mm) was selected for the alkali removal process (see Chapter 3).

$$\frac{\mathrm{E}}{[\frac{kWh}{t}]} = -41.8 \cdot \ln(\mathrm{d_p}) + 137.51 \qquad (79)$$

$$R^2 = 0.909$$

in which d_p is the maximum diameter of particle (mm)

Table 25. Some examples of energy consumption.

max d_p [mm]	E [kWh/t]
5	70
0.92	141

7 Cost evaluation

7. 1 Fixed capital investment

The purchase prices and the costs of the installed equipment are presented in Table 26. The installation factor is 0.1 for the most equipment (Hurme 2008), so the cost of installed equipment is calculated with Equation 80.

$$\text{Cost of installed equipment} = 1.1 \cdot \text{Purchase price} \quad (80)$$

Table 26 shows that the rotary vacuum drum washer, HA-1, is by far the most expensive equipment. The mechanical dewatering press, KE-1, is the second most expensive equipment and the HNO_3 storage tank, FA-6, is the third most expensive equipment. The cost of the installed equipment is about 40 % of the fixed capital investment (Hurme 2008). The estimation of the distribution of the fixed capital investment was found in Process Design Manual (Hurme 2008). It is illustrated in Table 27, which shows that the fixed capital investment of the process is about 5830 k€. It shows also that the installed equipment, engineering and supervision form the major part of the fixed capital investment.

Table 26. Purchase prices and costs of installed equipment.

Device ID	Name	Purchase price [k€]	Installed equipment [k€]	Share [%]
HA-1	Rotary vacuum drum washer	1100	1210	52
KE-1	Mechanical press	300.0	330.0	14
FA-6	HNO_3 storage tank	203	223	10
HX-1	Reverse osmosis - unit	78	85	4
FA-3	NaOH storage tank	56	62	3
GA-5A	Slurry feed pump	48.7	54	2
GA-5B	Slurry feed spare pump	48.7	54	2
GA-1A	Reverse osmosis feed pump	44	48	2
GA-1B	Reverse osmosis feed spare pump	44	48	2
GD-3	Slurry mixer	42.4	46.6	2
FA-4	Slurry mixing tank	42	46	2
EA-1	Heat exchanger for washing liquid	32	36	2
EA-2	Heat exchanger for water	32	36	2
FA-2	Tank	7.4	8.1	-
FA-1	Tank	6.9	7.6	-
GA-3A	Centrifugal pump	4.7	5.2	-
GA-3B	Centrifugal pump	4.7	5.2	-
GA-2A	Centrifugal pump	4.2	4.6	-
GA-2B	Centrifugal pump	4.2	4.6	-
FA-5	Tank	4.1	4.5	-
GA-4A	Centrifugal pump	3.7	4.1	-
GA-4B	Centrifugal pump	3.7	4.1	-
JD-1	Screw conveyor	2.8	3.1	-
JD-2	Screw conveyor	3.1	3.4	-
GD-1	Mixer	0.5	0.6	-
GD-2	Mixer	0.3	0.3	-
KA-1	Crusher	0	0	-
Total		2121	2334	100

Table 27. Distribution of fixed capital investment.

	[%]	[k€]
Installed equipment	40	2334
Engineering & supervision	20	1167
Piping	10	583
Building & HVAC	8	467
Instrumentation & controls	7	408
Insulation & painting	4	233
Site preparation	3	175
Start-up	3	175
Electrical	3	175
Structural steel	2	117
Total (Fixed capital investment)	100	5834

7.2 Operating costs

7.2.1 Fixed costs

The fixed costs consist of repair, maintenance, salaries, social costs, taxes, research, development, insurances, royalties and quality control in this case. Administration, rents and marketing were expected to be zero, because the unit is considered to be built and used in connection with an existing plant.

Repair and maintenance are 5–10 % of fixed capital investment (Sinnott 2005). In this case, they were evaluated to be 8 %, because the cleaning and changing of the reverse osmosis membranes are taken into account. The taxes are 2 %, insurances 1 % and royalties 1 % of the fixed capital investment (Sinnott 2005).

Five operators work in the uninterrupted three-shift job system. There is always one operator working at a time. The annual salary of one operator is 35000 €, so the monthly salary of an operator is 2900 €. The salaries and social costs altogether are evaluated to be 1.5 times higher, since the pension payments,

social securities, accident insurances, holiday bonuses, education, occupational health services, sick leaves and work clothes are taken into consideration.

Quality control is 20 % of salaries and social costs (R.K. Sinnott 2005). Research and development were evaluated to be 30 % of the salaries and social costs. Thus, two experts could be hired also: a laboratory assistant with a monthly salary of 2900 € and a M.Sc. with a monthly salary of 4350 €. As a result, the alkali removal unit would employ seven people.

7.2.2 Variable costs

The variable costs consist of the chemicals (HNO_3 and NaOH), water, waste water and electricity. They are calculated based on the balances and the power consumptions of equipment (see Chapter 6). They are presented in Table 29.

Electricity is required for the rotating, pressing, pumping, mixing and conveying. The cost of industrial electricity was 0.072 €/kWh in Finland in 2014 (Energy price statistics 2015). Spare pumps are seldom used, so they are not taken into consideration when calculating electricity. The electricity consumption of the unit is presented in Table 28. It shows that the reverse osmosis feed pump, GA-1A, has the largest consumption, followed by the mechanical press, KE-1.

Table 28. Electricity consumption of unit.

Device ID	Name	[kWh]	%
GA-1A	Reverse osmosis feed pump	160	38
KE-1	Mechanical press	130	31
GA-5A	Slurry feed pump	38	9
HA-1	Rotary vacuum drum washer	37.5	9
GD-3	Slurry mixer	22	5
GA-3A	Centrifugal pump	11	3
GA-2A	Centrifugal pump	7.5	2
GD-1	Mixer	3.4	0.8
GA-4A	Centrifugal pump	2.2	0.5
JD-2	Conveyor	2	0.5
GD-2	Mixer	1.8	0.4
JD-1	Conveyor	0.73	0.2
	Total	416	100.0

The price of 100 % sodium hydroxide is 0.288 €/kg (Alibaba 2016b). The price of 68 % nitric acid is 0.27 €/kg (Alibaba 2016a). The industrial water cost was evaluated to be 0.57 €/m^3, which is the industrial water cost in Neste Oil (Sundblom 2015). The waste water treatment cost in Joensuun vesi is 1.93 €/m^3 (Joensuun vesi 2016).

The typical operating time of a CHP-plant was evaluated to be 5500 h/a (Solantausta 2016). This was taken into consideration by multiplying all the variable costs with an operating time factor, which was calculated with Equation 81.

$$\text{Operating time factor} = \frac{\text{operating time}}{\text{the whole year}} \quad (81)$$

The moisture of the biomass is equal before and after the alkali removal unit (see Chapter 6.1.1). Thus, there is no increase or decrease in the drying costs before pyrolysis.

7.2.3 Conclusion

Operating costs consist of variable costs and fixed costs. The operating costs are presented in Table 29, which shows that nitric acid and sodium hydroxide correspond about 60 % of operating costs. Table 29 also shows that the operating costs of the process are 4469 k€/year.

Table 29. Operating costs.

Cost	Price [k€/a]	[%]
HNO_3	1812	41
NaOH	834	19
Waste water	432	10
Electricity	165	4
Water	133	3
Variable costs	3376	76
Repair and maintenance	467	10
Salaries and social costs	263	6
Taxes	117	3
R&D	79	2
Insurances	58	1
Royalties	58	1
Quality control	53	1
Fixed costs	1094	24
Total	4469	100

7.3 Sale incomes

The evaluation of the costs of a new process is relatively accurate, when compared to the estimation of the incomes. They fluctuate according to the customer interest, economic situation and product quality for example. Therefore, it is possible to present only a rough simplification in this thesis. It should be noted that the sale incomes are presented here for a case, in which 91

% of ash is removed and the product is sold in the price of light fuel oil. That is because the unit would not ever have paid itself back in the real case without major changes: the operating costs would have been higher than the sale incomes.

The current price of the fast pyrolysis bio-oil is similar to that of heavy fuel oil, after having considered the difference between their lower heating values. The lower heating values as MJ/kg (Solantausta 2016), prices €/kg (Nyyssönen 2016) and prices €/MJ are presented in Table 30. The LHV of the FPBO is 15.6, when the oil has about 24 % moisture (Solantausta 2016). Table 30 shows that the price of the new product would be 0.26 €/kg, which is 0.017 €/MJ, if it was sold in the similar price as light fuel oil €/MJ.

Table 30. The lower heating values and prices of the product

	unit	HFO	LFO	$FPBO_{old}$	$FPBO_{new}$
LHV	MJ/kg	41.1	42.7	15.6	15.6
Price	€/kg	0.49	0.72	0.19	0.26
	€/MJ	0.012	0.017	0.012	0.017

Due to the reduction of ash in the feed, a plant producing 48 500 t/a may be estimated to be able to increase its production to 56 300 t/a (Solantausta 2016). This is based on the assumption that the yield of the organic liquid is increased from 50 % to 58 % on dry basis (Oasmaa et al. 2015b), which is optimistic considering the results of the pyrolysis experiment in this thesis (see Chapter 4). Sale incomes were calculated with Equation 82. They are about 5790 k€/a.

$$\text{Sale incomes} = \mathrm{c_{New}} \cdot \mathrm{C_{New}} - c_{Old} \cdot \mathrm{C_{Old}} \quad (82)$$

In which c = capacity (kg/a) and C = cost (€/kg)

7.4 Profitability

The sale incomes are 5790 k€/a, if 91 % of ash was removed, the product sold in the price of light fuel oil and the yield of organic liquid increased from 50 % to 58 % on dry basis (see Chapter 7.3), fixed capital investment 5830 k€ (see Chapter 7.1) and the operating costs 4470 k€/a (see Chapter 7.2). The earnings before interest, taxes, depreciation and amortization, EBITDA, are about 1320 k€/a by Equation 83.

$$\text{EBITDA} = \text{sale incomes} - \text{operating costs} \quad (83)$$

The company tax percent was 20 % in Finland in 2015 (Veronmaksajain keskusliitto ry 2015). The profit of financial period, PFP, is about 1060 k€/a by Equation 84.

$$\text{PFP} = \text{EBITDA} - \text{taxes} = \text{EBITDA} - 0.2 \cdot \text{EBITDA} \quad (84)$$

The PFPs of future years are discounted to the present moment by multiplying them with the discounting factors. Those values are referred to as NPV of PFP*, (net present value of profit of financial period*) here. The discounting factors, f_d, are calculated from Equation 85. The required internal rate of return, IRR, is usually 15 % in Finnish companies (Golam 2016).

$$f_d = \left(1 + \left(\frac{\text{IRR}}{100}\right)\right)^{-n} \quad (85)$$

In n = year

Equation 86 shows that the return of investment, ROI, is the inverse number of the payback time, PBT.

$$\mathrm{ROI} = \left(\frac{1}{\mathrm{PBT}}\right) \cdot 100\ \% \qquad (86)$$

NPV of unit (*net present value of unit*) is the sum of the opposite number of the fixed capital investment and the positive values of the NPVs of PFPs. The right value for PBT is found from the point where the NPV of unit is zero.

This is illustrated in Figure 19. It shows that the PBT is 12.5 years, so ROI is 8.0 % according to Equation 92. Thus, the process does not have economic potential without major modifications. Table 31 presents the discounting factors, NPVs of PFPs and NPVs of unit.

Table 31. NPV values.

n	PFP	f_d	NPV of PFP	NPV of unit
0	-5834	1.00	-5834	-5834
1	1059	0.87	921	-4913
2	1059	0.76	801	-4112
3	1059	0.66	696	-3416
4	1059	0.57	605	-2811
5	1059	0.50	526	-2284
6	1059	0.43	458	-1827
7	1059	0.38	398	-1429
8	1059	0.33	346	-1083
9	1059	0.28	301	-782
10	1059	0.25	262	-520
11	1059	0.21	228	-292
12	1059	0.19	198	-94
13	1059	0.16	172	78

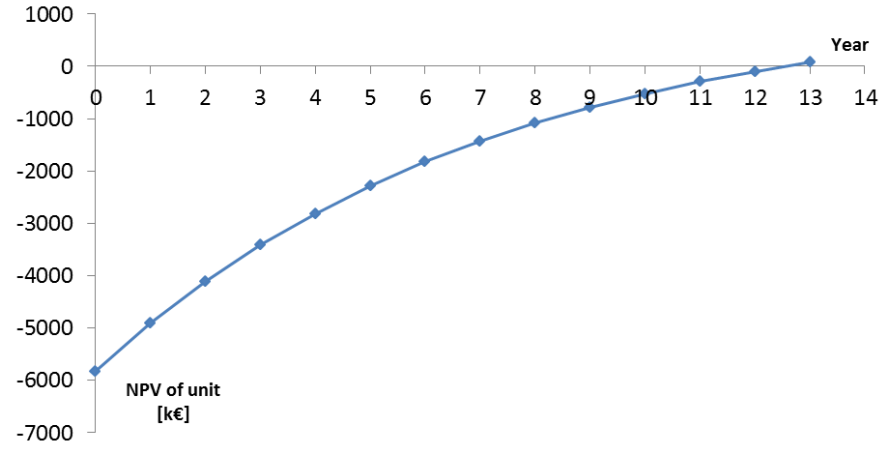

Figure 19. NPV of unit as function of time, if 91 % of ash was removed, the product sold in the price of light fuel oil and the yield of organic liquid increased from 50 % to 58 % on dry basis

7.5 Sensitivity analysis

Sensitivity analysis is a tool for viewing how the profitability of investment changes, when one or more parameters are changed. In this thesis, the sensitivity analysis was performed for the change in the fixed capital investment and the prices of the chemicals (HNO_3 and NaOH), which have the most significant impact on the operating costs (see Chapter 7.2.3). These factors affect the economic feasibility the most after the sale incomes, which instead could have not been increased any further. Own estimation for the economic feasibility of a new unit is presented in Table 32. It should be still noted that 91 % of ash is removed and product sold in price of light fuel oil in the base case of cost evaluation.

Table 32. Estimation for economic feasibility of a new unit

ROI	PBT	Feasibility
100	1	Extreme
50	2	Great
33	3	Good
25	4	Fine
20	5	Ok
<20	>5	No

The operating costs vary according to the change of the fixed capital investment. In the first part of the sensitivity analysis, only the fixed capital investment was changed. Table 33 presents the fixed capital investment and operating costs in this part. The sensitivity analysis of the fixed capital investment is presented in Figure 20. It shows that the payback time decreases to about 3.8 years, if the investment is reduced to 3500 k€.

Table 33. Fixed capital investment, FCI, and operating costs, OC, in first part of sensitivity analysis

FCI [k€]	OC [k€]
3500	4190
4500	4310
5830	4470

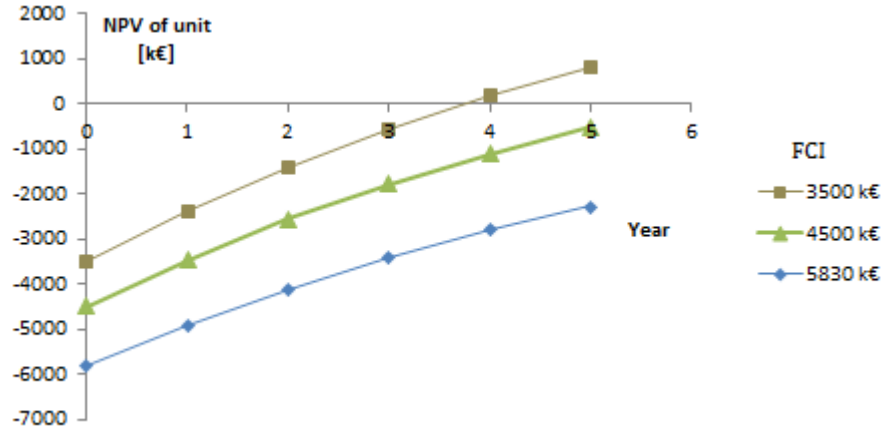

Figure 20. Sensitivity analysis of fixed capital investment

In the second part of the sensitivity analysis, only the prices of the chemicals (HNO_3 and NaOH) were changed. The sensitivity analysis of chemical prices is presented in Figure 21. It shows that the payback time is decreased to about 3.8 years, if the nitric acid and sodium hydroxide could be purchased half-price.

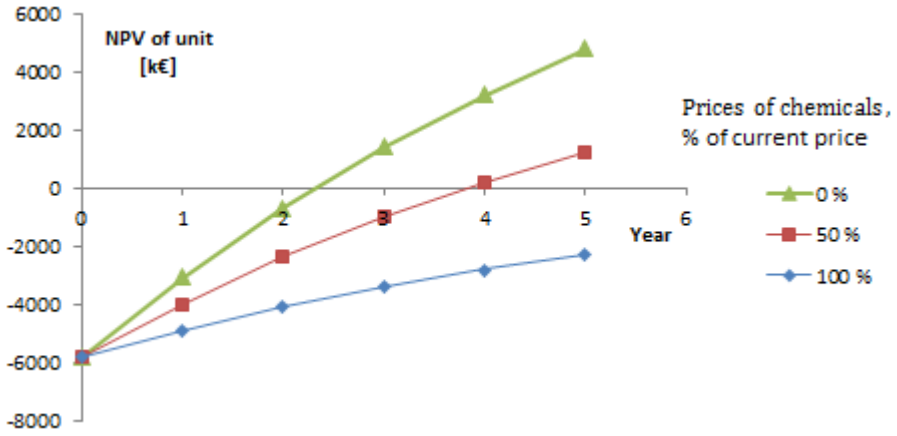

Figure 21. Sensitivity analysis of chemical (HNO_3 and NaOH) prices

If offering prices for these chemicals are available, the economic potential of the process would increase. The effect of the fixed capital investment on the economic potential should not be ignored either; the equipment suppliers should be selected carefully to avoid too high purchase prices.

8 Conclusions

8.1 Summary

There were two aims in this thesis. The first goal was to design a realistic and functioning biomass alkali removal process for the fast pyrolysis plant. Another objective was to study the economic potential of that process. The price of the fast pyrolysis bio-oil increases, when the alkalis are removed from the feed. This is mainly due to the organic liquid yield and product quality increase but also to the reduction in the particulate emissions.

The alkali removal unit was designed by testing the wash process in laboratory and pilot scale, choosing the suitable equipment, drawing the flow chart including the control instruments, calculating the mass balances, defining the most important technical values for all the equipment and writing the operating instructions. The economic potential of the new unit was studied by searching the current prices for all equipment, calculating the fixed capital investment, calculating the operating costs of the unit based on the balances and the power consumption of equipment. In addition, the sensitivity analysis was performed for the fixed capital investment and chemical prices.

Nitric acid was selected as the washing liquid based on the laboratory experiments, easy waste liquid treatment, supportive results in literature and possibility of good neutralization salt rejection by reverse osmosis. The optimal process conditions were defined according to the laboratory experiments. They are washing temperature 40 °C, rinsing water temperature 40 °C, residence time

0.5 h, nitric acid concentration 1 %, washing solution-biomass mass ratio 1:5, rinsing-water mass ratio 1:5 and the normal chip size (<5 mm). The goal for the removal efficiency of biomass ash was achieved in laboratory in the limitations of measurement accuracy and almost achieved in the pilot scale. The total ash removal was 50 % in laboratory and 45 % in pilot scale. The pilot scale experiment, however, was performed without the real equipment, so better removal efficiencies are expected in plant scale. Rotary vacuum drum washer is the washing equipment of choice, because of its relatively inexpensive price and well-known technique in the pulp industry. The pyrolysis experiment showed that the yield of the organic liquid was only slightly increased, when the washed biomass was used in pyrolysis instead of the regular forest residue. The yield was raised from 53 % to 56 % on dry basis.

This process was designed to be as simple, safe and environmentally friendly as possible. The inherent safety is very high due to many reasons: the amount of process devices is minimized, the used washing temperature (40 °C) is low, all the nitric acid is neutralized with the sodium hydroxide, the concentration of nitric acid and sodium hydroxide are low, the risk of corrosion is minimized, because almost all equipment is stainless steel, the storage tank sizes for nitric acid and sodium hydroxide are minimized, the equipment of choice is commonly used in the process industry and the process functions continuously. The dilute sodium hydroxide and nitric acid solutions do not evaporate at these conditions. The electricity consumption of the unit is relatively low, below 400 kWh, when the biomass feed is 4.6 kg/s.

The process is not economically feasible without major changes and further study. Even if 91 % of ash was removed, the product sold in the price of light fuel oil and the yield of organic liquid raised from 50 % to 58 % on dry basis, the payback time of the unit would have been 12.5 years. If only 50 % of ash was removed and the product sold in a more realistic price, the sale incomes would have been lower than the operational costs.

8.2 Recommendations for continuation

It is recommended to study experimentally the presented alternative more in detail. Particularly higher washing temperatures should be investigated, since good results have been indicated in literature (Oudenhoven et al. 2013, Oudenhoven et al. 2015). It is recommended to explore the chemistry of the washing process more in detail, such as the reactions of biomass and alkalis with nitric acid. A pilot experiment with the right equipment is strongly recommended. The quality of the product after the pyrolysis should be examined too, so that more accurate evaluation of its price was obtained. The other methods for the biomass alkali removal, such as hot-filtration of vapours, ion-exchange of bio-oil, filtration, centrifugation and steam explosion, are recommended to study too.

The possibility of using hydrochloric acid as the washing liquid could be examined as well. For this, the propensity of hydrochloric acid to destroy the structure of biomass should be tested in laboratory. The limits of the chlorides in the combustion and the risks of the chloride corrosion should be explored too. If hydrochloric acid was used as the washing liquid, the environmental friendliness of the unit would increase even further; the only waste flow would consist of just water, table salt and ash compounds.

More experimental data is required on the moisture content of the biomass after the novel mechanical dewatering press. The moisture could be decreased more in the pressing, if the slight damage of the structure of the biomass and the need for a higher pressure were not obstacles. Then the large drying costs in the fast pyrolysis plant would be decreased. There could be actually a possibility to test the press in Karlstad (Sobota 2016). The possibility of manufacturing fertilizer of the waste water flow could be studied. That flow has 2.8 % sodium nitrate and 0.6 % other ash compounds, and the flow rate of 41 tons/hour. The salts could be separated with an additional reverse osmosis and subsequent evaporation units.

References

Alakangas E. 2000. Suomessa käytettävien polttoaineiden ominaisuuksia, VTT tiedotteita 2045, VTT Valtion Teknillinen Tutkimuskeskus, Espoo

Alibaba, 2016a. Big factory price of nitric acid, cited 22.3.2016, Available at: http://www.alibaba.com/product-detail/-Big-Factory-price-of-nitric_1923516818.html?spm=a2700.7724857.29.1.TCCnCL&s=p

Alibaba, 2016b. Hot-Selling High Quality Low Price NaOH 99, cited 21.4.2016, Available at: http://www.alibaba.com/product-detail/Hot-Selling-High-Quality-Low-Price_60268961502.html?spm=a2700.7724857.0.0.Q2fqi3&s=p

Alibaba, 2016c. Hydrochloric acid, cited 20.4.2016, Available at: http://www.alibaba.com/product-detail/hydrochloric-acid-factory-manufacture-and-sale_60063348692.html?spm=a2700.7724857.29.46.xmfOuE

Alibaba, 2016d. 99.3 % Sodium nitrate price, white prilled sodium nitrate with top quality, cited 2.5.2016, Available at: http://www.alibaba.com/product-detail/99-3-sodium-nitrate-price-white_60445775699.html?spm=a2700.7724857.29.3.oU3bex&s=p

Alopaeus V., Ke-42-1700 Kemian laitetekniikka I, Osa 4 Aineensiirto ja erotusprosessit, Cited 26.1.2016. Available at: https://noppabackup.aalto.fi/noppa/kurssi/ke-42.1700/materiaali/KE-42_1700_prujut_4.pdf

Anonymous, 2016. Rahanarvonlaskuri. Cited 13.4.2016. Available at: http://apps.rahamuseo.fi/rahanarvolaskin#FIN

Averill B., Eldredge P., 2016. General Chemistry: Principles, Patterns, and Applications, v. 1.0 (2 Volume Set), Flat World Education, Inc., Chapter 13.4, Effects of Temperature and Pressure on Solubility

Baird L., Muller S., Freel B., 2015. Methods and Apparatuses for Forming Low-metal Biomass-derived Pyrolysis Oil, United States Patent, US8940060 B2

Biermann, C., 1996. Handbook of Pulping and Papermaking, Second Edition, pp. 24–27

Bradley D., 2015. Pyrolysis Oil – Commercial Markets are a Reality, Lee enterprises consulting inc, Cited 29.2.2016. Available at: http://lee-enterprises.com/pyrolysis-oil-commercial-markets-are-a-reality/

Bradshaw J., 1997. Source Book of Alternative Technologies for Freshwater Augmentation in Latin America and the Caribbean, Chapter 2.1, Desalination by Reverse Osmosis

Bridgwater, A.V. Meier, D. Radlein D., 1999. An overview of fast pyrolysis of biomass. *Organic Geochemistry*, 30, pp. 1479–1493

Dalluge D., Daugard T., Johnston P., Kuzhiyil N., Wright M., Brown R., 2014. Continuous production of sugars from pyrolysis of acid infused lignocellulosic biomass, *Green Chem*, 16, 4144-4155

Datta S., Lin Y.J., Snyder S.W., 2014. Advances in Biorefineries, Biomass and Waste Supply Chain Exploitation, Chapter 5, pp. 112–151

Davidsson K.O., Korsgren J.G., Pettersson J.B.C., Jäglid U., 2002. The effects of fuel washing techniques on alkali release from biomass, *Fuel*, 81, pp. 137-142.

Dow (a), Filmtec™ Membranes, Product Information, FT30 Reverse Osmosis Membrane Specifications, Form No. 609-01020-0406, Cited 5.4.2016

Dow (b), Filmtec™ BW30-365 Element, Product Data Sheet, Form No. 609-00153, Cited 15.4.2016.

Empyro, Energy & materials from pyrolysis, 2015. Cited 29.2.2016. Available at: http://www.empyroproject.eu/index.php

Energy Price Statistics. 2015. Statistics Explained. Cited 25.1.2016. Available at: http://ec.europa.eu/eurostat/statistics-explained/index.php/Energy_price_statistics

The Engineering Tool Box (a). Salinity of Water. Cited 22.2.2016. Available at: http://www.engineeringtoolbox.com/water-salinity-d_1251.html

The Engineering Tool Box (b). Overall Heat Transfer Coefficient. Cited 15.4.2016. Available at: http://www.engineeringtoolbox.com/overall-heat-transfer-coefficient-d_434.html

Fortum, 2015. Energy Production. Fuel. Bio oil. Cited 4.1.2016. Available at: http://www.fortum.com/en/products-and-services/biooil/pages/default.aspx

Fusion Express, 2016. Impellers, Pitch Blade Turbine (PBT) Impeller, Cited 12.4.2016, Available at: http://www.fusion-express.com/impellers-pitch-blade-turbine#/pageSize=1000&viewMode=list&orderBy=0&pageNumber=1

GL&V, 2014. Vacuum Washer. Cited 26.1.2016. Available at: http://www.glvpulppaper.com/pulp/Washing/VacuumWasher/Coru-DekVVacuumCylinder

Golam S., D.Sc., Lecturer in the Department of Plant Design, University of Aalto, personal contact 31.5.2016

Heikkilä T., Expert of Sulzer Finland Pumps, consulted 22.3.2016.

Hurme M., 2008. Process Design Manual, 1st Edition

Icis, Part of rbi *(reed business information)*. Chemical profile: nitric acid, Relx Group™, cited 12.5.2016, Available at: http://www.icis.com/resources/news/2008/05/19/9124327/chemical-profile-nitric-acid/

Insee, 2016. National Institute of Statistics and Economic Studies, Measuring, understanding, cited 29.2.2016, Available at: http://www.insee.fr/en/bases-de-donnees/bsweb/serie.asp?idbank=001642885

Jacob, A. Expert Toray Membrane Europe AG Switzerland, consulted 15.4.2016

Jiménez S., Ballester J., 2006. Particulate Matter Formation and Emission in the Combustion of Different Pulverized Biomass Fuels. *Combustion Science and Technology*, 178 (4), pp. 655–683.

Joensuun vesi. 2016. Asiakkaalle. Cited 12.1.2016. Available at: http://www.joensuunvesi.fi/documents/1368623/1761394/Laatuvaatimukset+asumaj%C3%A4tevesist%C3%A4%20poikkeaville+j%C3%A4tevesille/e6461ebe-1d95-488f-aecb-b7bbb1a07d46

Jussila T., GL&V Pulp & Paper Expert, contacted 26.5.2016

Kaipainen M., 2003. Männyn, kuusen ja koivun kemiallinen koostumus, Pro gradu-tutkielma ja erikoistyö

Karkela L., Meriläinen P., 2011. Maol taulukot. Kemia. 2.–9. Painos. Otavan Kirjapaino Oy, pp. 135, 147

Kaukoranta K., Joensuun vesi. Advising on telephone 10.2.2016

Keskinen K.I., 2004. Kemian laitetekniikan taulukoita ja piirroksia, 10. muuttumaton painos, 845, Otatieto, ISBN 951-672-069-2

Koskinen A., Aalto University Professor of Organic Chemistry, consulted 10.2.2016

Kuzhiyil N., Dalluge D., Bai X., Ho Kim K., Brown R., 2012. Pyrolytic Sugars from Cellulosic Biomass, *ChemSusChem*, 5 (11), 2228-2236

Kyllönen H., Senior Scientist VTT Jyväskylä, consulted 5.4.2016

Laine J., Sales Manager, Uutechnic, tel. +358 284 688 30. Personal contact 31.5.2016

Lindfors C., Research Scientist, VTT, personal contact 23.6.2016

Loh H. P. et at, 2002. Process Equipment Cost Estimation Final Report, *Netl*, p. 17 Spiral Plate Heat Exchanger, DOE/NETL-2002/1169

Material Safety datasheets of the condensate compounds (MSDS)

McCabe S. and H., Unit Operations of Chemical Engineering, 5th Edition, Chapter 26 Membrane Separation Processes, Reverse Osmosis, pp. 871–878

Melin, K. Senior Scientist at VTT, personal contact 12.5.2016

Mourant D., Wang Z., He M., Wang XS., Garcia-Perez M., Ling K., Li C., 2011. Mallee wood fast pyrolysis: effects of alkali and alkaline earth metallic species on the yield and composition of bio-oil, *Fuel*, 90, 9, 2915-2922

Mynewsdesk, 2014. Presentation of world-wide unique dewatering press. Cited 2.2.2016. Available at: http://www.mynewsdesk.com/se/paperprovince/pressreleases/presentation-of-world-wide-unique-dewatering-press-1100267

Nyyssönen S., Research Scientist, VTT, Engines and emissions, contacted 9.2.2016.

Oasmaa A., Principal Scientist, VTT, contacted 20.1.2016

Oasmaa A., Sundqvist T., Kuoppala E., Garcia-Perez M., Solantausta Y., Lindfors C., Paasikallio V., 2015a. Controlling the phase stability of biomass fast pyrolysis bio-oils: American Chemical Society. *Energy and Fuels,* Vol. 29, No. 7, pp. 4373-4381

Oasmaa A., Solantausta Y., Lehto J., Lindfors C., Reinikainen M., Källi A., Paasikallio V., Onarheim K., 2015b. Transportation fuel production within existing

bioenergy and mineral oil industries through integrated biomass pyrolysis – 2G biofuels. Research report, VTT-R-03852-13, Chapter 3.5.2 Solids and alkali metals, pp. 28–29

Oasmaa A., Solantausta Y., Arpiainen V., Kuoppala E., Sipilä K., 2010a. Fast Pyrolysis Bio-Oils from Wood and Agricultural Residues. *Energy and Fuels*, No. 24, pp. 1380-1388, Available at: http://pubs.acs.org/doi/pdf/10.1021/ef901107f

Oasmaa A., Peacocke C., 2010b. A guide to physical property characterization of biomass-derived fast pyrolysis liquids. A guide. VTT Publications: 731, Espoo, VTT, 79 p. + app. 46 p. ISBN 978-951-38-7384-4. Available at: http://www.vtt.fi/inf/pdf/publications/2010/P731.pdf

Oinas, P. CHEM-E7105 Process Development, Lecture 1, Cited 25.2.2016, Available at: https://mycourses.aalto.fi/mod/folder/view.php?id=97206

Outotec, 2016. Outotec Larox Pressure Filters. Cited 22.01.2016. Available at: http://www.outotec.com/en/Products--services/Process-equipment/Filters/Pressure-filters/

Oudenhoven S.R.G., Westerhof R.J.M., Aldenkamp N., Brilman D.W.F., Kersten S.R.A., 2013. Demineralization of wood using wood-derived acid: Towards a selective pyrolysis process for fuel and chemicals production. *Journal of analytical and Applied Pyrolysis*, 103, pp. 112–118.

Oudenhoven S.R.G., Westerhof R.J.M, Kersten S.R.A., 2015. Fast pyrolysis of organic acid leached wood, straw, hay and bagasse: Improved oil and sugar yields. *Journal of analytical and Applied Pyrolysis*, 116, pp. 253–262

Paasikallio V., Lindfors C., Kuoppala E., Solantausta Y., Oasmaa A., Lehto J., Lehtonen J., 2014. Product quality and catalyst deactivation in a four day catalytic fast pyrolysis production run. *Green Chemistry*

Paasonen, E. Research Technician, VTT. Personal contact 2016.

Page J.S., 1996. Conceptual cost estimating manual (2nd edition). Section 2 Process Equipment, Conveying equipment, screw conveyors p.85

Partanen, M. Pump expert in AxFlow Helsinki, personal contact 26.4.2016

Puretec. Basics of Reverse Osmosis. Cited 15.4.2016, Available at: http://puretecwater.com/resources/basics-of-reverse-osmosis.pdf

Scholze B., Long-term Stability, Catalytic Upgrading, and Application of Pyrolysis Oil, Improving the Properties of a Potential Substitute for Fossil Fuel, Dissertation, Hamburg, 2002

Seminarsonly, 2015. Mechanical Projects. Rotary Drum Vacuum Filter. Cited 1.2.2016. Available at: http://www.seminarsonly.com/Engineering-Projects/Mechanical/Rotary_Drum_Vacuum_Filter.php

Sinnott, R. K., 2005. Chemical Engineering Design, Coulson & Richardson's Chemical Engineering, Volume 6, Fourth Edition, pp. 267

Sinnott, R., Towler G., 2013. Chemical Engineering Design – Principles, Practice and Economics of Plant and Process Design, Chapter 18.3.4.2 Screw Conveyors, 2nd edition, pp. 962

Sobota E.S.G, Originator and financier of the dewatering press, Copolia SA, phone +41 78 912 88 65. Personal contact, 30.5.2016.

Sobota E.S.G., Karlsson C.J.I., 2014. An apparatus and a method for dewatering wood chips. Copolia Company, Patent WO2014033156 A1

Solantausta, Y. Senior Principal Scientist, Principal Investigator, VTT. Personal contact 2016

Solantausta Y., Oasmaa A., Sipilä K., Lindfors C., Lehto J., Autio J., Jokela P., Alin J., Heiskanen J., 2012. Bio-oil Production from Biomass: Steps towards Demonstration. *Energy & Fuels,* 26, pp. 233-240

Steele A., 2015. Advanced Plumbing Technology, Chapter 8

Stefanidis S.D., Heracleous E., Patiaka D.T., Kalogiannis K.G., Michailof C.M, Lappas A.A., 2015. Optimization of bio-oil yields by demineralization of low quality biomass. *Biomass and Bioenergy*, 83, pp. 105–115

Sundblom S., expert in catalyst characterization, Neste Oil Research and Development, consulted 14.4.2015

Tarleton, S. Wakeman R., 2007. Solid/Liquid Separation – Equipment Selection and Process Design, Chapter 1 and Chapter 7

Taulukot.com, 2016. Hapot, emäkset, pH – Happovakioita, cited 2.5.2016. Available at: http://www.taulukot.com/index2.php?search_id=hapot&lng=fi

Tech Fact, Dow membranetec membranes, Form no. 609-00240-0311, Cited 26.2.2016, Available at: http://msdssearch.dow.com/PublishedLiteratureDOWCOM/dh_0660/0901b8038066098e.pdf?filepath=liquidseps/pdfs/noreg/609-00240.pdf&fromPage=GetDoc

Thelander, A. Drinor dewatering press expert, consulted 30.3.2016

Tilastokeskus, 2015. Energian hinnat. ISSN=1799-7984. 3. Vuosineljännes 2015, Liitekuvio 2. Tärkeimpien öljytuotteiden kuluttajahinnat. Helsinki: Tilastokeskus. Cited 29.2.2016. Available at: http://tilastokeskus.fi/til/ehi/2015/03/ehi_2015_03_2015-12-14_kuv_002_fi.html

Trendewicz A., Evans R., Dutta A., Sykes R., Carpenter D., Braun R., 2015. Evaluating the effect of potassium on cellulose pyrolysis reaction kinetics. *Biomass and bioenergy*, 74, pp. 15-25.

Turn S. Q., Kinoshita C.M., Ishimura D.M., 1997. Removal of inorganic constituents of biomass feedstocks by mechanical dewatering and leaching. *Biomass and Bioenergy*, 12, pp. 241-252.

Valmari, T., 2000. Potassium behavior during combustion of wood in circulating fluidized bed power plants. VTT Publications 414, ISBN 951-38-5569-4, pp. 21

Veronmaksajain keskusliitto ry., 2015. Yritysveroprosentit EU-maissa. Cited 12.4.2016. Available at: https://www.veronmaksajat.fi/luvut/Tilastot/Tuloverot/Yhteisoverotus/

Vassilev S.V., Baxter D., Andersen L.K., Vassileva C.G., Morgan T.J., 2012. An overview of the organic and inorganic phase composition of biomass. *Fuel*, 94, 1–33

Vuori A., CHEM-E7105 Process Development, Lecture 8, Cited 12.4.2016, Available at: https://mycourses.aalto.fi/mod/folder/view.php?id=97206

Couper J.R., Penney W.R., Fair J.R., Walas S.M., 2012. Chemical Process Equipment – Selection and Design, 3rd edition, Chapter 5.3.2 Screw Conveyors, pp. 71

Watson-Marlow, Bredel Hose Pumps, Bredel 265, Bredel 280 and Bredel 2100 hose pumps, cited 27.4.2016, Available at: http://www.watson-marlow.com/Documents/knowledge-hub/Datasheets/gb%20-%20UK/Bredel%20rebrand/wd-bredel_265_280_2100-gb-03.pdf

Wikberg A., Senior Lead Engineer, Etteplan, +46 730 338 963. Personal contact 30.5.2016

Wilén C., Moilanen A. Kurkela E., 1996. Biomass feedstock analyses, VTT Publications 282, ISBN 951-38-4940-6

Attachment 1. Flow rates and mass concentrations

	Total	Ash	Ash	$NaNO_3$	$NaNO_3$	HNO_3	HNO_3	NaOH	NaOH	
Flow no	[t/h]	[g/s]	[ppm]	[g/s]	[%]	[g/s]	[%]	[g/s]	[%]	pH
1	20.3	0	0	0	0	340	4.1	0	0	0.2
2	16.6	148	32000	0	0	0	0	0	0	7
3	149.4	75	1800	10	0.023	340	0.6	0	0	1.1
4	40	72	6510	311	2.8	0	0	0	0	7
5	45.8	1	67	4	0	0	0	0	0	7
6	0.7	0	67	0	0	0	0	0	0	7
7	40.7	72	6400	311	2.8	0	0	0	0	7
8	33.2	75	8160	0	0	0	0	0	0	7
9	9.6	0	0	0	0	0	0	0	0	7
10	10.5	0	0	0	0	0	0	150	5	14.1
11	159.9	75	1680	320	0.7	0	0	0	0	7
12	83	1	59	6	0.026	0	0	0	0	7
13	37.2	0	0	0	0	340	2.2	0	0	0.4
14	73.4	1	67	6	0.029	0	0	0	0	7
15	16.3	75	16580	0	0	0	0	0	0	7
16	16.9	0	0	0	0	0	0	0	0	7
17	83	1	37	4	0.016	340	1	0	0	0.8
18	1.2	0	0	0	0	340	68	0	0	-1.2
19	19.1	0	0	0	0	0	0	0	0	0
20	99.6	148	5360	4	0.013	340	0.8	0	0	0.9
21	0.5	0	0	0	0	0	0	0.15	100	15.7
22	10.0	0	0	0	0	0	0	0	0	0
23	119.9	2	67	10	0.029	0	0	0	0	0
24	124.4	0	0	0	0	0	0	0	0	7
25	124.4	0	0	0	0	0	0	0	0	7
26	124.4	0	0	0	0	0	0	0	0	7
27	124.4	0	0	0	0	0	0	0	0	7

Attachment 2. Flow chart

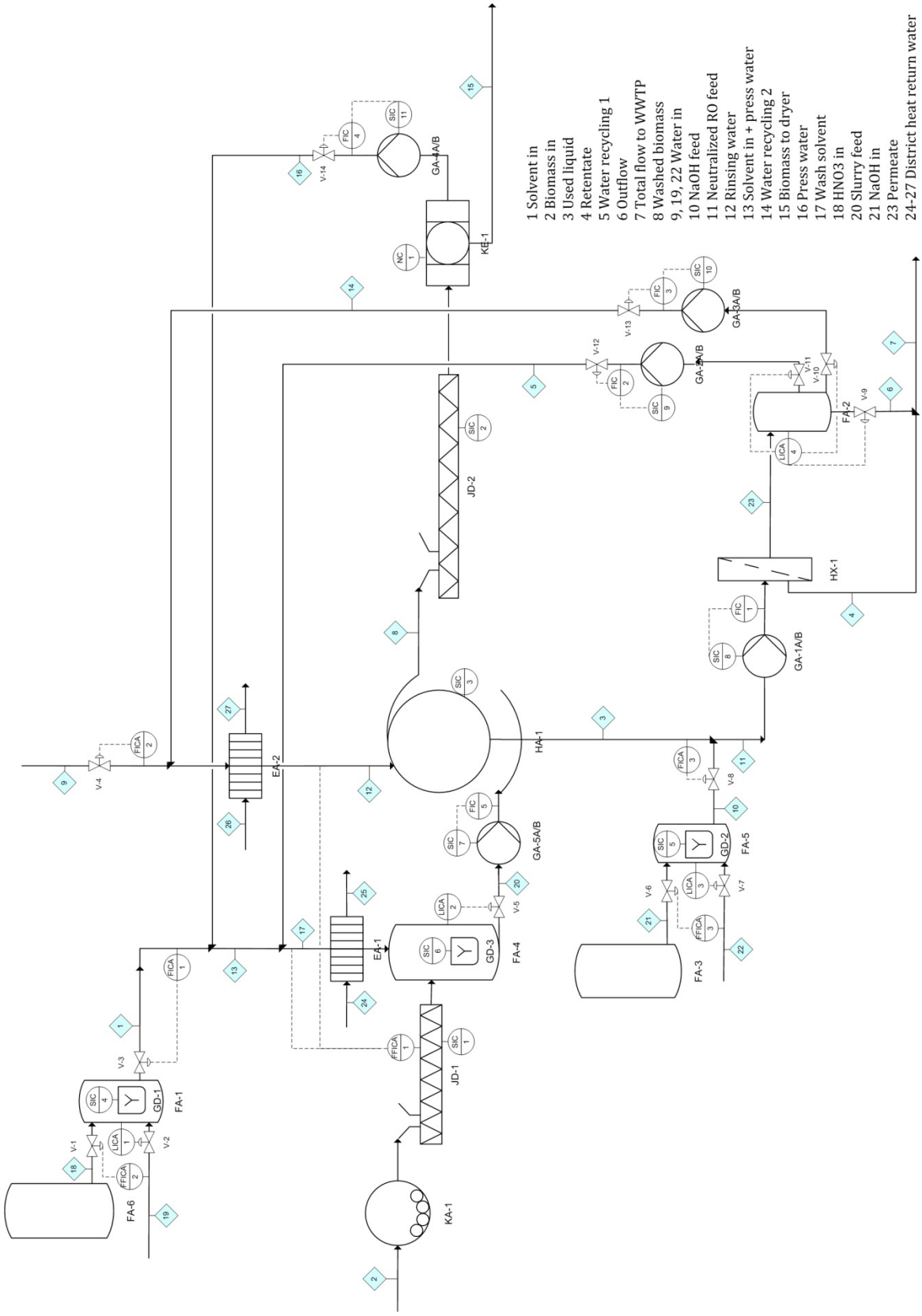

Attachment 3. Properties of condensate at VTT

(VTT data, MSDS)	Condensate [w-%]	Condensate organics [w-%]	Tb [°C]	Properties	Chemical formula	Reaction with AAEM ions possible (Koskinen 2016)
Water	73.7					
Acetaldehyde	5.35	20.3	21	Extremely flammable	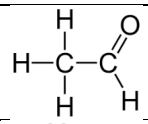	
Methanol	4.17	15.8	65	Easily flammable, toxic	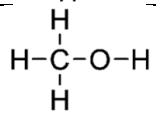	X
Acetic acid	2.53	9.6	118	Flammable, corrosive	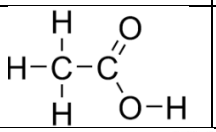	X
n-Propanol	1.13	4.3	82	Flammable, toxic	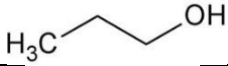	
Acetone	1.08	4.1	56	Easily flammable	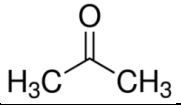	
1-Hydroxy-2-propanone	1.01	3.8	146	Flammable	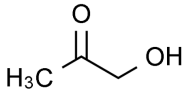	X
Furan	0.92	3.5	31	Extremely flammable	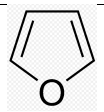	
Isopropanol	0.79	3.0	82	Highly flammable	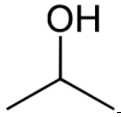	
Formic acid	0.40	1.5	101	Highly flammable	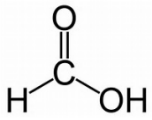	X
Furfural	0.33	1.3	162	Toxic	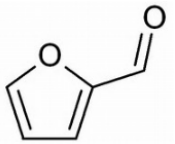	
n-Propionic acid	0.17	0.6	142	Flammable	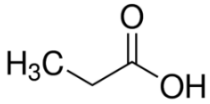	X
Others*	0.11	0.5				
"Sugars"	1.75	6.7				
Unidentified	6.6	25.0				
Total	100.0	100.0				

* Others include guaiacol, ethanol, 5-methylfurfural and phenol.

Attachment 4. Compounds of ash in biomass

(Vassilev et al. 2012)

3. Inorganic matter	
3.1. Silicates	
Albite	$NaAlSi_3O_8$
Augite	$(Ca,Na)(Mg,Fe,Al,Ti)(Si,Al)_2O_6$
Biotite	$K(MgFe)_3AlSi_3O_{10}(OHF)_2$
Chlorite	$(MgFe)_5Al_2Si_3O_{10}(OH)_8$
Clay minerals	K—Na—Ca—Mg—Fe aluminosilicates
Cristobalite	SiO_2
Cs silicate	
Diopside	$CaMg(SiO_3)_2$
Feldspars	$NaAlSi_3O_8$—$CaAl_2Si_2O_8$, $KAlSi_3O_8$
Forsterite	Mg_2SiO_4
Illite	$(K,H_2O)Al_2(Al,Si)Si_3O_{10}(OH)_2$
Kaolinite	$Al_2Si_2O_5(OH)_4$
K feldspar	$KAlSi_3O_8$
Mg aluminosilicates	
Montmorillonite	$(NaCa)_{0.3}(AlMgFe)_2Si_4O_{10}(OH)_2{\cdot}xH_2O$
Muscovite	$KAl_2AlSi_3O_{10}(OH)_2$
Opal (amorphous or crystalline, silicic acid polymerised, biogenic silica, silica phytolith)	$SiO_2{\cdot}nH_2O$
Orthoclase	$KAlSi_3O_8$
Plagioclases	$NaAlSi_3O_8$—$CaAl_2Si_2O_8$
Quartz	SiO_2
Sepiolite	$Mg_8H_6Si_{12}O_{30}(OH)_{40}(H_2O)_8$
Talc	$Mg_3Si_4O_{10}(OH)_2$
Vermiculite	$(MgFeAl)_3(SiAl)_4O_{10}(OH)_2{\cdot}4H_2O$
Wollastonite	$Ca_3Si_3O_9$
Zeolites	$(Ca,Sr,Ba,Na_2,K_2)\ Al_2Si_{2-10}O_{8-24}{\cdot}2–8H_2O$
3.2. Oxides and hydroxides	
Al hydroxide	$Al(OH)_3$
Al oxides	
Brucite	$Mg(OH)_2$
Corundum	Al_2O_3
Cu—Al oxides	
Cu—Fe oxide	
Fe oxide	
Goethite	α-FeOOH
Hematite	Fe_2O_3
Magnetite	$FeFe_2O_4$
Ni oxide	
Portlandite	$Ca(OH)_2$
Rutile	TiO_2
Sn oxide	
Spinels	$MgAl_2O_4$—$Mg(AlFe)_2O_4$
Zn oxide	
Zn—Mn oxide	

3.3. Sulphates, sulphites and sulphides	
Anhydrite	$CaSO_4$
Arcanite	K_2SO_4
Barite	$BaSO_4$
Ettringite	$Ca_6Al_2(SO_4)_3(OH)_{12}{\cdot}26H_2O$
Fe sulphate	$Fe_2(SO_4)_3$
Fe—Zn sulphide	
Gypsum	$CaSO_4{\cdot}2H_2O$
Jarosite	$KFe_3(SO_4)_2(OH)_6$
Millosevichite	$Al_2(SO_4)_3$
Pyrite	FeS_2
Thenardite	Na_2SO_4
Sulphides	Compounds with sulphide anion (S^{2-})
Sulphites	Compounds with sulphite anion (SO_3^{2-})
Zn sulphide	
3.4. Phosphates	
Apatite	$Ca_5(PO_4)_3(F,Cl,OH)$ or $Ca(PO_4)_3(F,Cl,OH)$
Fe phosphate	$FePO_4$
Hydroxyl-apatite	$Ca(PO_4)_3(OH)$
K hydrogen and K dihydrogen phosphates	K_2HPO_4, KH_2PO_4
Mg—Ca phosphate	$MgCaPO_4$
Mn phosphate	
3.5. Carbonates	
Ankerite	$Ca(MgFe)(CO_3)_2$
Calcite	$CaCO_3$
Dolomite	$CaMg(CO_3)_2$
K—Na—Ca—Mg carbonates	
Magnesite (Fe-rich)	$(Mg,Fe)CO_3$
3.6. Chlorides	
Bi chloride	
Halite	NaCl
K—Ca chloride	
K perchlorate	$KClO_4$
Sylvite	KCl
3.7. Nitrates	
Ca nitrate dihydrate	$Ca(NO_3)_2{\cdot}2H_2O$
Nitrates	
Nitre (niter)	KNO_3
Nitrocalcite	$Ca(NO_3)_2{\cdot}4H_2O$
3.8. Other inorganic matter	
Au—Ni phase	
Bi-bearing phase	
Glass	Various elements
Metallic alloys and pure metals	Various elements
Native Au, Fe, Mn and Zn	
Ni—Fe—As phases	

Attachment 5. Separation efficiency of RO for some alkalis

Compound *(Source: Tech Fact 2016)*	Separation efficiency [%]
Sodium Orthophosphate	99
Sodium Acetate (1 %)	88
Sodium Bicarbonate	98
Sodium Chloride	99
Sodium Di-H Phosphate	98
Sodium Hydrogen Sulphate	76
Sodium Mono-H Phosphate	98
Sodium Nitrate	93–98
Calcium Chloride	99
Calcium Nitrate	95
Magnesium Chloride	98
Magnesium Sulphate	99

Attachment 6. List of control instruments

Control instrument abbreviation	Control target	Control device	Measuring point
FFICA-1	Biomass feed	JD-1	Flow 17, Flow 12
FFICA-2	Strong HNO_3 feed	V-1	Water to FA-1
FFICA-3	Strong NaOH feed	V-6	Water to FA-5
FICA-1	Dilute HNO_3 feed	V-3	Flow 1
FICA-2	Water feed	V-4	Flow 9
FICA-3	Dilute NaOH feed	V-8	Flow 3
LICA-1	Water feed to FA-1	V-2	FA-1
LICA-2	Slurry feed to GA-5	V-5	FA-4
LICA-3	Water feed to FA-5	V-7	FA-5
LICA-4	Flow rates 5, 6, 14	V-9, V-10, V-11	FA-2
SIC-8	GA-1 power	FIC-1	FIC-1
SIC-9	GA-2 power	FIC-2	V-12
SIC-10	GA-3 power	FIC-3	V-13
SIC-11	GA-4 power	FIC-4	V-14
SIC-7	GA-5 power	FIC-5	FIC-5
NC-6	KE-1 power	KE-1	KE-1
SIC-1	JD-1 rotating speed	JD-1	JD-1
SIC-2	JD-2 rotating speed	JD-2	JD-2
SIC-3	HA-1 rotating speed	HA-1	HA-1
SIC-4	GD-1 rotating speed	GD-1	GD-1
SIC-5	GD-2 rotating speed	GD-2	GD-2
SIC-6	GD-3 rotating speed	GD-3	GD-3